ELECTROCHEMICAL STUDIES ON TRANSITION METAL OXIDES WITH ELECTRONIC CONDUCTIVITY

YASUMICHI MATSUMOTO

JANUARY, 1977

ELECTROCHEMICAL STUDIES ON TRANSITION METAL OXIDES WITH ELECTRONIC CONDUCTIVITY

YASUMICHI MATSUMOTO

JANUARY, 1977

PREFACE

The work in this thesis was performed under the guidance by Professor Hideo Tamura at the Department of Applied Chemistry, Faculty of Engineering, Osaka University.

Yasumichi Matsumoto

Suita, Osaka
January, 1977

CONTENTS

CHAPTER I

GENERAL INTRODUCTION

In the prediction of energy shortage in the new future, importance of developing fuel cells has been rerecognized. Up to now, a variety of investigation on fuel cell systems have been conducted, and choise of oxygen electrode as the cathode of fuel cells has been recognized to be the most-promising for a practical goal. It may be said, therefore, that electrochemical reduction of oxygen has become one of the most important process for electrochemical energy conversion. However, as far as our present knowlege concerns, only expensive catalyst, such as platinum, are believed to be effective in the oxygen electrode of the fuel cell.

In recent years, several papers have been published, in which some transition metal oxides have a promising character for electro-catalyst for oxygen reduction. However, the nature of the catalysis of these oxides for oxygen reduction has not yet been clarified at all. In order to find out a good electro-catalyst, it is very valuable to clarify the nature of the electrocatalysis of these oxides. If one makes a success in elucidating the catalytic nature which is common to almost all the transition metal oxides, he can know in advance what

kind of oxide is effective as a catalyst for oxygen reduction.

From the above point of view, present work has been coducted to find out the nature of the catalytic property which is common to a variety of the transition metal oxides. For this purpose, it was necessary to expand my research on a variety of transition metal oxides, the electrochemical properties of which have not yet been studied. As a matter of course, the some electrochemical properties of these oxides have been investigated.

The contents of this thesis are mainly composed of the following papers.

1) A New Catalyst for Cathodic Reduction of Oxygen: Lanthanum Nickel Oxide,
   Y. Matsumoto, H. Yoneyama and H. Tamura,
   Chem. Lett., 661 (1975)
2) Electrochemical Properties of Lanthanum Nickel Oxide,
   Y. Matsumoto, H. Yoneyama and H. Tamura,
   J. Electroanal. Chem., in press.
3) Catalytic Activity for Electrochemical Reduction of Oxygen of Lanthanum Nickel Oxide and Related Oxides,
   Y. Matsumoto, H. Yoneyama and H. Tamura,
   J. Electroanal. Chem., in press.

4) Influence of Preparation Condition on Catalytic Activity for Oxygen Reduction of Lanthanum Nickel Oxide and Related Oxides,

Y. Matsumoto, H. Yoneyama and H. Tamura,

J. Electroanal. Chem., in press.

5) Influence of the Nature of the Conduction Band of Transition Metal Oxides on Catalytic Activity for Oxygen Reduction,

Y. Matsumoto, H. Yoneyama and H. Tamura,

J. Electroanal. Chem., in press.

6) Dependency of the Exchange Current Density of Oxygen Reduction on the Resistivities of $La_{1-x}Sr_xMnO_3$ and $LaNi_{1-x}M_xO_3$ Electrodes,

Y. Matsumoto, H. Yoneyama and H. Tamura,

J. Electroanal. Chem., in press.

CHAPTER II

ELECTROCHEMICAL PROPERTIES OF SEVERAL TRANSITION METAL OXIDES WITH HIGH ELECTRICAL CONDUCTIVITY.

II - 1. INTRODUCTION

It is well recognized that in general, oxygen ions in oxides with the perovskite type structure are mobile [1, 2]. From an electrochemical point of view, it is a matter of question whether such the transition metal oxides with the perovskite type structure keeps its original composition by appreciable polarization at potentials covering oxygen reduction. Surface characterization of the transition metal oxides are, therefore, required before the electrocatalytic properties of the oxides for oxygen reduction are studied in detail.

In this chapter, basic electrochemical properties of the transition metal oxides with a high electrical conductivity, such as the perovskite type oxide, $LaNiO_3$, $LaTiO_3$, $SrVO_3$, $SrRuO_3$, $SrFeO_3$ and $La_{1-x}Sr_xMnO_3$, as well as the corundom type oxide, $V_{0.2}Ti_{1.8}O_3$, are studied. Among them, $LaNiO_3$ is studied in detail.

II - 2. EXPERIMENTAL

$LaTiO_3$. $SrVO_3$, $SrRuO_3$, $La_{1-x}Sr_xMnO_3$ and $V_{0.2}Ti_{1.8}O_3$ were synthesized by similar methods to those described by Kestigian et al. [3], Chamberland et al. [4], Callagham et al. [5], Jonker [6] and Kawakubo et al. [7], respectively. $LaNiO_3$ was synthesized at 850°C for 2 days in air by using La_2O_3 and NiO as the starting materials and by Na_2CO_3 as the flux. The sample prepared was thoroughly washed with distilled water and then dried at 100°C [8]. $SrFeO_3$ was synthesized at 1200°C for 4-5 hours in air by using $SrCO_3$ and Fe_2O_3 as the starting materials [9]. This oxide presumably contained small amount of oxygen ion vacancy as reported by MacChesney [9]. In all the synthesis, starting materials were pressed into a tablet form with $100Kgcm^{-2}$ The identification of the substances produced was made by x-ray diffraction analysis. The specific resistivities were measured by the four probe method. $LaTiO_3$, $SrVO_3$, $SrRuO_3$, and $V_{0.2}Ti_{1.8}O_3$ could be synthesized to give firm sintered discs. Then they were used as the electrode merely being water-proofed with polystyrene. In the case of $SrFeO_3$ and $La_{1-x}Sr_xMnO_3$, however, the oxides were not so firmly sintered when they were prepared, and the powder form was obtained in the case of $LaNiO_3$. $SrFeO_3$ and $La_{1-x}Sr_xMnO_3$ were crushed to powder with an agate mortar. The powdered oxides were mixed with Afron (Co-polymer of tetrafluoro-

ethylene and ethylene) as a binder with weight ratio 7 : 1 and pressed with 100 $Kgcm^{-2}$ into tablet form (1mm thick x 13mm dia.). These specimens were heated at 250°C and then water-proofed by polystyrene. The specimens prepared by this way gave reproducible results. The both end of surfaces of the two kinds of the specimens, i.e., sintered and pressed pellets were polished with #2000 emery papers, and an electrical lead was connected via silver paste on the one side of the surfaces. The specimen was then mounted in a glass tube with epoxy resin.

Specific resistivities of sintered discs of $LaTiO_3$, $SrFeO_3$, $SrVO_3$, $SrRuO_3$, $V_{0.2}Ti_{1.8}O_3$ and $La_{1-x}Sr_xMnO_3$ were 1.2, 5.0×10^{-1} 6.0×10^{-3} 9.4×10^{-4} 4.0×10^{-4} and $3.0\sim8.0\times10^{-2}$ Ωcm respectively, while a pressed pellets of $LaNiO_3$ with binder gave a specific resistivity of 0.8 Ωcm.

The electrolytes of 1N-NaOH and 1N-H_2SO_4 were pre-electrolyzed for five days. The potential sweep method was employed to study the basic polarization behaviors of the electrode itself with a sweep rate of 10 $mVsec^{-1}$ Resistive and capasitive components of the $LaNiO_3$ electrode were obtained as a function of the electrode potential by means of a wheastone bridge assembly already reported [10]. All measurements were made at 25°C.

Amounts of total nickel ions and Ni^{3+} ions in lanthanum nickel oxide were determined by the same

manner as that described by Wold et al. [8]. The amount of Ni^{2+} ions was determined by subtraction of the amount of Ni^{3+} ions from that of total ions. The amount of oxygen ions was determined by calculation so as to give electrical neutrality of the oxide. Lanthanum nickel oxide prepared in this study had a composition of $LaNi^{3+}_{0.67}Ni^{2+}_{0.33}O_{2.84}$. However, the composition of this oxide is expressed in this thesis as $LaNiO_3$ for simplicity in description.

II - 3. RESULTS AND DISCUSSION

II - 3 - 1. Lanthanum nickel oxide

1N-NaOH solution was used as electrolyte in the case of $LaNiO_3$, since this oxide dissolves immediately upon immersion in acid solutions. Fig. 1 shows typical

Figure 1

voltammograms of $LaNiO_3$ electrode in 1N-NaOH. When the voltammogram was taken in a restricted potential region between 0.6 and 0 V, a couple of oxidation and reduction peaks appeared as the curves (a) shows, while a potential sweep in a wide potential region gave the curve (b), showing that the redox peaks became broad. Results by chemical analysis of the electrode before and after a constant potential electrolysis at -0.8 V for ten hrs, which are presented in Table 1, showed that trivalent

Table 1

nickel ions were reduced to bivalent ions by the electrolysis. In the table, the result after the electrolysis is given as if the composition change progressed homogeneously through the entire electrode, although it might not be the case. The charge consumed during the electrolysis is given in third column of the table, and in the fouth

column, calculated charge necessary for the composition change determined is given. The values of them are roughly in accord with each other. From this result, the cathodic current in the potential region less noble than -0.3 V is attributable to reduction of Ni^{3+} in the crystal to Ni^{2+}. The reverse reaction on the anodic sweep seems to proceed in the potentials anodic to 0.6 V in this case. The couple of the redox peaks which appeared in the potential region in the curve (a) can then be assigned to the redox reaction of Ni^{4+}/Ni^{3+}.

X ray analysis was made to the electrode surface before and after the constant potential electrolysis at -0.8 V. Diffraction peaks of (110) and (012) planes of the oxide became ambiguous by the reduction. This result suggests that a little destruction of the crystal structure was brought about by the cathodic reduction. The Ni^{2+} ions produced by the reduction of Ni^{3+} will be unable to occupy their original sites without any deformation of the lattice, because the atomic radius of Ni^{2+} is larger than that of Ni^{3+}. This is possibly the main reason for the crystal destruction. After the electrolysis, the crystal increased its resistivity by two orders of magnitude ($\sim$100 Ωcm).

Fig. 2 shows potential/time curves of the electrode when it was polarized at 400 μAcm^{-2} and the open circuit

potential decays at various stage of the E/t curves. The

Figure 2

E/t curve in the reduction was obtained after the electrode was oxydized with the constant current of 400 $\mu A cm^{-2}$ for ten minutes. The plateaus of B and B' correspond to the couple of the redox reactions of Ni^{4+}/Ni^{3+}.

At the end of the plateau B' in Fig. 2, i.e., at the point (f), composition of the electrode surface is judged to be $LaNi^{3+}O_3$, because at this stage, reduction of Ni^{4+} to Ni^{3+} is completed. Therefore, it is possible to determine composition of the oxidized electrode by analyzing a quantity of electricity of the plateau B: For this purpose, an electrode was prepared by the same manner as that reported by Kudo et al. [2], that is a few drops of 1N-NaOH solution was added to mixture of acetylene blak 0.025 g, graphite 0.025 g and lanthanum nickel oxide 0.5 g, and then the mixture was mounted in an acryle frame with the same construction as that shown in Fig. 3 of ref. [2]. In this structure of the electrode, almost all the surface of the oxide particles charged is expected to be available for electrochemical oxidation. After the prepared electrode was oxidized at a fixed current density for five to ten hrs in an oxygen evolution condition, the electrode was reduced

with the same current density. As for the current density, various values less than 1 $mAcm^{-2}$ were chosen. The shape of the potential/time curve was similar to that shown in Fig. 2. If the composition of the fully oxidized electrode is presented as $LaNiO_{3+\delta}$, the value determined by analysis of the quantity of electricity of the plateau B' was 0.001, regardless of oxidation time and current density chosen. The charge to bring the change of δ=0.001 roughly corresponds to five to seven times the charge necessary for oxidation of monolayer of $LaNi^{3+}O_3$ to $LaNi^{4+}O_{3.5}$, if the reaction area is assumed to be the same as the BET surface area, i.e., 0.56 m^2g^{-1} However, whether the oxidation proceeded in the restricted surface of a few monolayer or not is not clear. From a point of crystal geometry, it seems unlikely to impregnate oxygen into the crystal in such a high concentration as to give $LaNi^{4+}O_{3.5}$. Consequently, oxidation reaction may have propagated into a deeper interior of the crystal. Anyway, the result shows that the redox reaction

$$LaNiO_3 + 2\delta OH^- \rightleftharpoons LaNiO_{3+\delta} + 2\delta e$$

is likely, although the reaction is quite limited in the surface region of electrode.

As is shown in Fig. 2, the open circuit potential of the electrode changed slowly with time after current interrupter in such a manner that it decreased during

the oxidation and increased during the reduction. The behavior is quite similar to that observed on other oxide electrodes, such as manganese dioxide [11], nickel oxide [12] and $La_{1-x}Sr_xCoO_3$ [2], and is connected to the ionic diffusion in the surface of oxide electrode, which brings rearrangement of ions in the surface region after current interruption. In the case of lanthanum nickel oxide, the species responsible for the open circuit decay is possibly oxygen ions as in the case of $La_{1-x}Sr_xCoO_3$ [2].

Fig. 3 shows resistive and capacitive components

Figure 3

of the electrode as a function of the electrode potential. The measurements were made at first cathodically from 0 to -1.2 V at which the polarization direction was reversed. All the points in the figure were obtained at a metastable state which was attained after polarization for about five to ten minutes. The resistance of the electrode showed a marked dependency on electrode potentials and became low with polarization toward a noble direction, although a noticeable hysterisis was observed in the both components. High resistance of the electrode in less noble potentials is in accord with the result obtained by the resistivity measurements by

the four probe method on the electrode before and after the constant potential electrolysis at -0.8 V, which already described in an above section.

The conductivity of lanthanum nickel oxide is due to σ^* band formation of the atomic orbitals of nickel and oxygen [13]. Concentration of oxygen ion in the crystal changes depending on valency change of nickel in the crystal. If the oxygen vacancies in the oxide increase by reducing Ni^{3+} to Ni^{2+}, then the degree of the interaction will decrease, resulting in an increase in resistivity. On the contrary, the resistance of the electrode surface must become low in the high anodic potential region, because the concentration of oxygen ion in the oxide becomes high at the high potential region. Such a result has already been reported for $Ln_{1-x}Sr_xCoO_3$ [14].

It is noticed that hysterisis appeared in the capacitive and resistive components. Once when the electrode was oxidized at a high anodic potential, it gave high capacitance and low resistance in the potential region between 0.4 V and -0.6 V compared with those at the electrode pre-reduced at less noble potentials. This result suggests that the more trivalent ions were retained in a inner surface region once when the electrode was polarized at a very high anodic potential. Though the hysterisis appeared, it is

confirmed by comparing behavior of the capacitive and resistive components with the voltammogram shown in Fig. 1-(b), that the redox reactions of Ni^{3+}/Ni^{2+} of the electrode proceed in the potential showing no distinct peak in the voltammogram.

II - 3 - 2. Some transition metal oxides with high electrical conductivity

Voltammograms of the other oxides obtained in 1N-H_2SO_4

Figure 4

Figure 5

and 1N-NaOH, are shown in Figs. 4 and 5. In the case of 1N-H_2SO_4, a distinct waves of the electrochemical reaction of the oxide itself was observable only for $SrVO_3$ and $SrRuO_3$. By the electrolysis of these oxides for several ten minutes at the potential giving the anodic peak current, the electrolyte turned light brown in the case of $SrRuO_3$, while in the case of $SrVO_3$, V^{5+} ion was detected in the electrolyte by a color identification using α-benzoin oxim. These results show that the anodic dissolution took place at the potential of the anodic peak current. In the case of 1N-NaOH, it was found that $SrRuO_3$, $LaTiO_3$ and $La_{0.8}Sr_{0.2}MnO_3$ were electrochemically active as shown in Fig. 5. On the other hand, the voltammogram of $SrFeO_3$ had a similar

shape to that of $LaTiO_3$ but the reaction current of the former was small compared with that of the latter. $V_{0.2}Ti_{1.8}O_3$ was quite stable. It was confirmed that any dissolution of the oxide did not occur at the potentials giving the current waves in the voltammograms in Fig. 5. Similar electrochemical reactions to that of $La_{0.8}Sr_{0.2}MnO_3$ were observed for $La_{1-x}Sr_xMnO_3$ having x=0, 0.1, 0.3 and 0.4, though the magnitude of the currents were diffrent depending on x. If one takes into consideration that all the oxides except for $V_{0.2}Ti_{1.8}O_3$ have the perovkite structure, the following conclusion is drawn that the redox reaction of the oxide itself readily occurs in alkaline solution in the surface reagion of the oxide. The redox reactions will be represented in general by the following equations by taking into account of analysis of the voltammograms of $LaNiO_3$ and of the Pourbeix diagrams.

$$ABO_3 + 2\delta_1 OH^- \rightleftharpoons ABO_{3+\delta_1} + \delta_1 H_2O + 2\delta_1 e \quad (1)$$

$$ABO_{3-\delta_2} + 2\delta_2 OH^- \rightleftharpoons ABO_3 + \delta_2 H_2O + 2\delta_2 e \quad (2)$$

where A is lanthanoid or alkaline earth ion and B is transition metal ion, δ_1 and δ_2 represent the excess and the deficiency of oxygen from the stoichiometric composition of the perovskite type oxides. Judging from the Pourbeix diagram and the positions of the current peaks of the voltammograms, only the reaction (2) seemed to occur in the cases of $LaTiO_3$, $SrFeO_3$,

$La_{1-x}Sr_xMnO_3$ and $SrVO_3$, while the both reactions of eqs. (1) and (2) seem to progress in the case of $SrRuO_3$, which is described in the chapter III.

TABLE 1. Change in composition of lanthanum nickel oxide by cathodic polarization at -0.8V for 10 hrs.

Composition before being electrolyzed	Composition after being electrolyzed	Coulomb obs.	Coulomb calc.
$LaNi^{3+}_{0.67}Ni^{2+}_{0.33}O_{2.84}$	$LaNi^{3+}_{0.57}Ni^{2+}_{0.43}O_{2.79}$	27.4	24.1

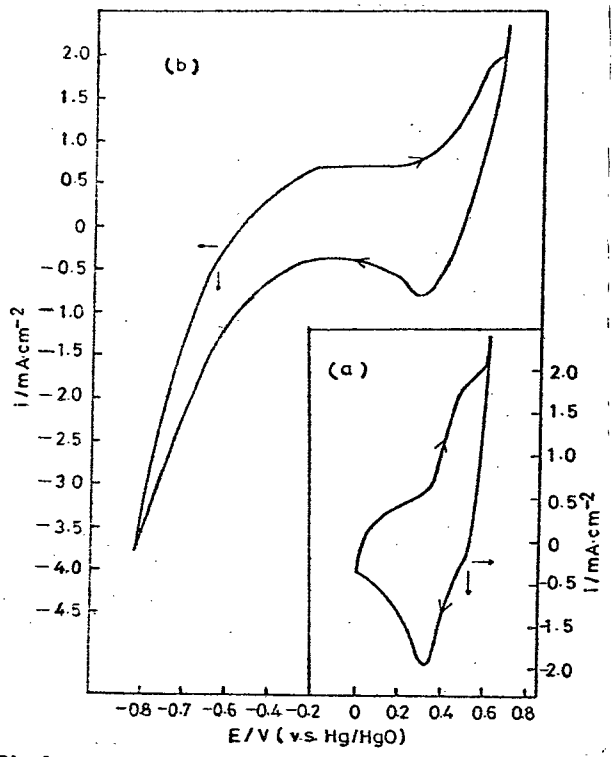

Fig.1. Potential sweep voltammograms of $LaNiO_3$ in 1N-NaOH.

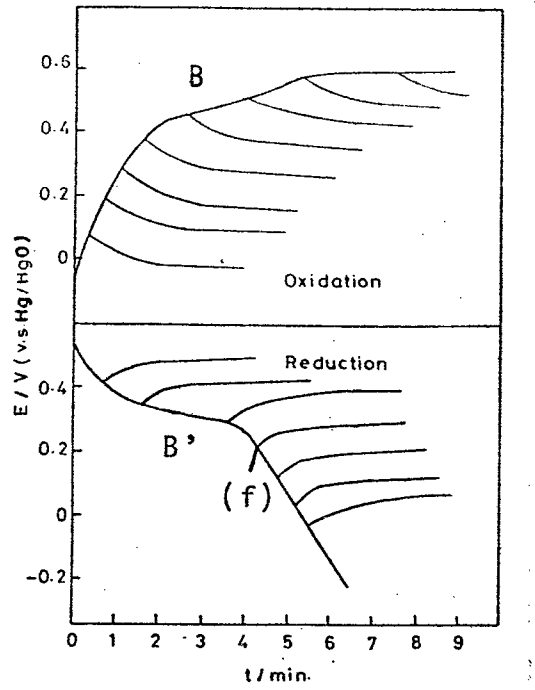

Fig.2. Open circuit potential decays of $LaNiO_3$ electrode polarized in various degrees by a constant current density of 400 $\mu Acm.^{-2}$

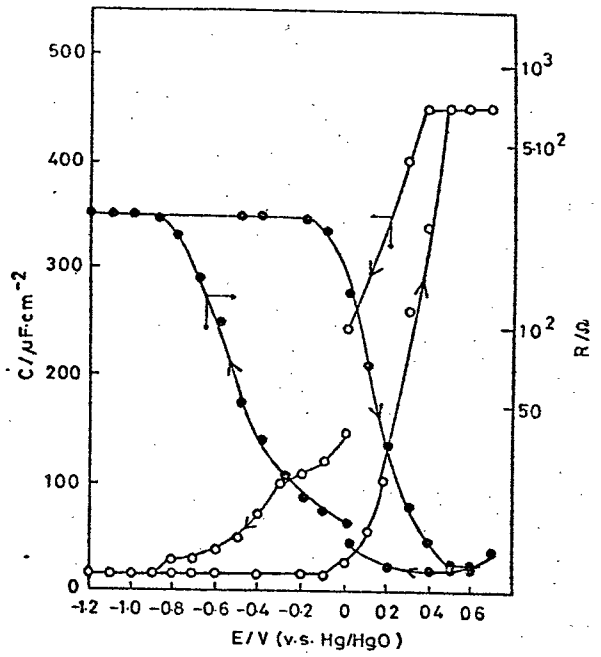

Fig.3. Differential capacitance and resistance of $LaNiO_3$ electrode in 1N-NaOH at 1KHz. (○) differential capacitance, (●) resistance.

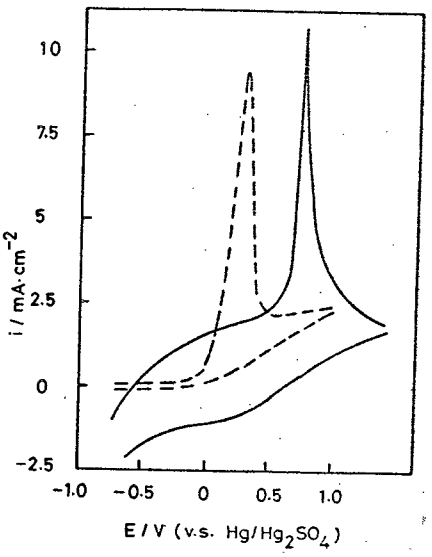

Fig.4. Potential sweep voltammograms in 1N-H_2SO_4. (———) $SrRuO_3$, (- - - - -) $SrVO_3$.

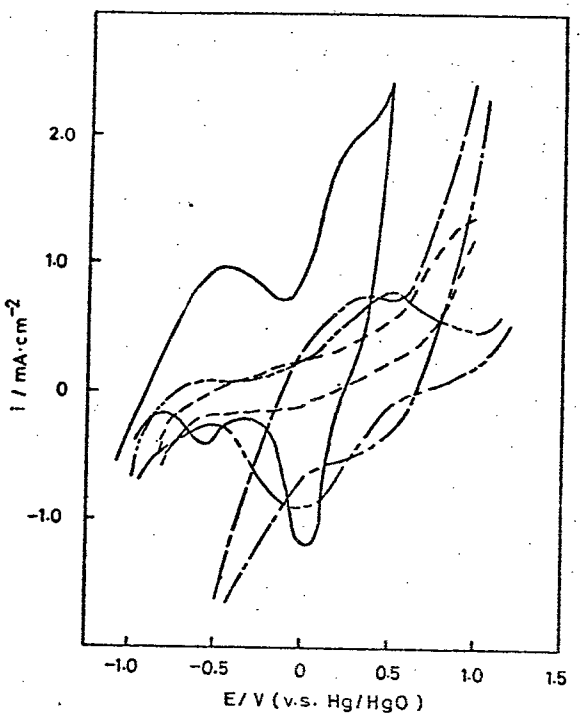

Fig.5. Potential sweep voltammograms in 1N-NaOH.
(———) $SrRuO_3$, (– – – –) $SrVO_3$, (— — —) $La_{0.8}Sr_{0.2}MnO_3$,
(— – — –) $LaTiO_3$.

CHAPTER III

INFLUENCE OF THE NATURE OF THE CONDUCTION BAND OF TRANSITION METAL OXIDES ON CATALYTIC ACTIVITY FOR OXYGEN REDUCTION

III - 1. INTRODUCTION

Several kinds of transition metal oxides such as Pt-doped tungsten bronze [15], Li doped NiO [16-18], $La_{0.5}Sr_{0.5}CoO_3$ [19] and $NiCo_2O_4$ [20,21] were reported to have a promising property as an catalyst for oxygen reduction. However, the main factor that controls the catalytic activity of these transition metal oxides has not yet been clarified.

The main purpose of this chapter is to elucidate the factor which controlls the catalytic activity. For this purpose, the catalytic activities of some oxides with a high conductivity such as $LaTiO_3$, $SrFeO_3$, $SrVO_3$, $SrRuO_3$, $V_{0.2}Ti_{1.8}O_3$, $LaNi_{1-x}M_xO_3$ (M: V, Co, Fe) and $La_{1-x}Sr_xMnO_3$ were investigated, and they as well as the catalytic activities of other oxides which were already reported, are compared with one another and discussed from the point of their nature of the conduction band.

III - 2. EXPERIMENTAL

Metallic oxides such as La_2O_3, NiO, CoO, Fe_2O_3 and V_2O_3 were used as the starting materials to prepare $LaNi_{1-x}M_xO_3$ (M: V, Co, Fe). The manner of the preparation of samples was same as that of $LaNiO_3$ which was described in the former chapter. The scanning rate of $2\theta^{o}min^{-1}=0.5$ was chosen in the case of the determination of the lattice constant by x ray analysis. Steady state polarization curves were obtained in the electrolyte into which oxygen gas was bubling. IR-free current/potential curves were obtained by using a current interrupter. All the measurments were conducted at $25^{o}C$. The other details have been described in the former chapter.

III - 3. RESULTS AND DISCUSSION

III - 3 - 1. Physical properties of oxides

According to Wold [8], $LaNiO_3$ belongs to the space group D3d(5)-R$\bar{3}$m, and lattice constants of the crystal having a hexagonal form are a=5.456 Å, c=13.122 Å. The lattice constants of the perovskite oxide are shown in Fig. 1 as a function of the degree of substitution, x. Dimension of the c axis

Figure 1

of $LaNiO_3$ prepared was 13.18 Å and larger than that reported by Wold. This difference may be due to different conditions of preparation such as temperature and preparation time (Wold chose 800°C for three days, while a condition of 850°C for two days was chosen in this present study). As figure shows, the lattice constants did not vary with x in the case of $LaNi_{1-x}Co_xO_3$. Considering that the dimension of the pseudocell of $LaNiO_3$ is almost the same as that of $LaCoO_3$, the radius of Ni^{3+} ion must be almost the same as that of Co^{3+} ion (0.56 Å) [22] in this perovskite type structure.

The invariance of the lattice constants in the case of $LaNi_{1-x}Co_xO_3$, therefore, possibly reflects that Ni^{3+} and Co^{3+} ions have the same ionic radius in the oxides. On the other hand, in the case of $LaNi_{1-x}Fe_xO_3$, the lattice constants of both the a and c axises increased with increase of the degree of substitution, indicating that the Vegard's law held good, although the value of the a axis did not increase beyond x=0.3. Taking into the fact that the ionic radius of Fe^{3+} ion (0.628 Å) is larger than that of Co^{3+} ion in the perovskite structure [22], it is quite reasonable for the lattice constants of $LaNi_{1-x}Fe_xO_3$ to increase with increase of x. The lattice constants of $LaNi_{0.9}V_{0.1}O_3$ were almost the same as those of $LaNi_{0.9}Fe_{0.1}O_3$. However, when trails were made to prepare $LaNi_{1-x}V_xO_3$ having more than x=0.2, a mixture of produced perovskite oxide and the starting materials were obtained. The failure to prepare single phase of perovskite for $LaNi_{1-x}V_xO_3$ with high degree

of substitution is unpredictable from the point of ionic radius of V^{3+}(0.625 Å) [22], which lies between those of Co^{3+} and Fe^{3+}. However, there is a possibility by thermodynamics that V^{3+} ions in $LaNi_{1-x}V_xO_3$ change into V^{5+} ions by the following reaction.

$$2Ni^{3+} + V^{3+} \rightleftharpoons 2Ni^{2+} + V^{5+}$$

If the total radii of the produced ions, i.e., Ni^{2+} and V^{5+}, are larger than those of the reactant ions, i.e., Ni^{3+} and V^{3+}, then the crystal will expand with increase of x so greatly that it cannot exist as the single phase of perovskite. On the other hand, in the case of $La_{1-x}Sr_xMnO_3$, the lattice constant varied scarcely with the amount of the substitution of strontium.

Resistivities of $La_{1-x}Sr_xMnO_3$ are shown in Fig. 2

Figure 2

as a function of the degree of substitution of strontium, x. When the resistivity was obtained for a sintered discs, it was fairly close to the value reported by Jonker [6]. The oxide disc with Afron binder (12.5 wt%), which was used as the electrode, had a very large resistivity. As shown in this figure, the tendency of the change of the resistivities as a function of x, however, were

almost the same in both cases, as expected. When the degree of substitution with strontium, x, becomes large, a localyzed e_g orbital of the transition metal ion in the oxide becomes available to form the σ^* band with an oxygen ion [13]. Simultaneously the width of the σ^* band becomes great. The decrease of the resistivity with an increase of x in the range of x=0 to 0.3, therefore, seems to be due to a decrease of the effective mass of electrons, m^*, which brings an increase of the mobility of electrons in the σ^* band, though physical significance of the increase of the resistivity at x=0.4 is not clear.

Fig. 3 shows specific resistivities of $LaNi_{1-x}M_xO_3$

Figure 3

with Afron binder (12.5 %), which was used as the electrode, as a function of the degree of substitution. In the case of $LaNi_{1-x}Fe_xO_3$ and $LaNi_{1-x}Co_xO_3$, the resistivities increased semilogarithmically with an increase of x and the degree of the increase was larger for $LaNi_{1-x}Fe_xO_3$ than for $LaNi_{1-x}Co_xO_3$. If comparison is made on the resistivities of each oxide with x=0.1, we see the following order of the resistivities;

$LaNiO_3 \approx LaNi_{0.9}V_{0.1}O_3 < LaNi_{0.9}Co_{0.1}O_3 < LaNi_{0.9}Fe_{0.1}O_3$

When the σ^* band is formed by overlapping the sp_σ orbital of oxygen ion and the e_g orbital of a transition metal ion, relations of the overlap integral, Δ^{σ}_{cac}, to the

critical overlap integral, Δ_c, are as follows [13]. $\Delta^{\sigma}_{cac} > \Delta_c$ for $LaNiO_3$ and $LaVO_3$, $\Delta^{\sigma}_{cac} \approx \Delta_c$ for $LaCoO_3$, and $\Delta^{\sigma}_{cac} < \Delta_c$ for $LaFeO_3$. Experimental results on the resistivities of $LaNi_{1-x}M_xO_3$ agree well with the order of magnitude of the overlap integral. Therefore, the conductivity seems to be determined solely by the overlap integral. The logarithmic dependency of the resistivity on the degree of substitution, which is observed in $LaNi_{1-x}Co_xO_3$ and $LaNi_{1-x}Fe_xO_3$, is connected to the prediction that the σ^* band becomes narrow with an increase of x. As a result, the effective mass m^* of electrons in the σ^* band increases with an increase of x, leading to low mobility of electron in this band.

III - 3 - 2. Electrocatalytic property for oxygen reduction

By comparing potential sweep voltammograms in Figs. 1 and 5 shown in the former chapter with steady state polarization curves of oxygen reduction, which are shown in Figs. 4, 5, 6 and 7, it is noticed

Figure 4

Figure 5

Figure 6

Figure 7

that the electrode surface of $LaNi_{1-x}M_xO_3$, $SrVO_3$ and $La_{1-x}Sr_xMnO_3$ might be slightly reduced during the measurements of the polarization curves of oxygen reduction. However, the reduction, if any, is believed to bring no detrimental composition change in the electrode surface. In the case of $SrRuO_3$, the polarization behavior of the electrode was found to be quite analogous to that of $LaNiO_3$. Therefore, the two distinct current peaks seem to be connected to a couple of the reactions of Ru^{3+}/Ru^{4+} and Ru^{4+}/Ru^{5+} to give $SrRuO_{3-\delta}$ and $SrRuO_{3+\delta}$, respectively. It follows from this identification of the peaks that the oxygen reduction proceeded in potentials to bring no distinct change in the surface composition of the electrode.

From polarization curves for oxygen reduction on $LaNi_{1-x}M_xO_3$ presented in Figs. 4 and 5, it is found that the order of the activity was $LaNiO_3 \approx LaNi_{0.9}V_{0.1}O_3 > LaNi_{1-x}Co_xO_3 > LaNi_{1-x}Fe_xO_3$ as far as the degree of substitution ranged between 0.1 and 0.3, and that the current densities decreased with an increase of x in both $LaNi_{1-x}Co_xO_3$ and $LaNi_{1-x}Fe_xO_3$. The decrease in the reduction current density of oxygen can be attributed to difference in the surface area of the electrode, because the surface areas of $LaNi_{1-x}M_xO_3$ (M: Co, Fe) was independent of the degree of substitution, and had the following values when it is expressed in m^2g^{-1}; $LaNiO_3$: 0.56, $LaNi_{0.9}Co_{0.1}O_3$:

0.45, $LaNi_{0.8}Co_{0.2}O_3$: 0.48, $LaNi_{0.7}Co_{0.3}O_3$: 0.43, $LaNi_{0.9}Fe_{0.1}O_3$: 0.37, $LaNi_{0.8}Fe_{0.2}O_3$: 0.44, $LaNi_{0.7}Fe_{0.3}O_3$: 0.36.

The important view of the electrocatalysis connected with the present study is the one proposed by Binder et al. [23,24], that the transition metal ions in the surface must have an empty d_z2 orbital and filled d_{xy}, d_{xz} in order for the oxides to have high catalytic activity for oxygen reduction. If their view is applicable to the present cases, $LaNi_{1-x}Fe_xO_3$ and $LaNi_{1-x}Co_xO_3$ must show as high activities as $LaNiO_3$, because back-donation of an electron from Fe^{3+} or Co^{3+} to oxygen should be as easy as that from Ni^{3+}. Experimental results were against this prediction. Consequently, we need an another view on electrocatalysis on these transition metal oxides.

In the case of the polarization curves of oxygen reduction on $La_{1-x}Sr_xMnO_3$ shown in Fig. 6, the current density increased with an increase of the degree of substitution with strontium, x. Again the increasing tendency of the reduction current of oxygen with an increase of x cannot be attributed to difference in the surface area of the electrode, because $La_{1-x}Sr_xMnO_3$ had the surface area of $1.0 \sim 1.2$ m^2g^{-1} independent of the degree of substitution.

From the both results of $LaNi_{1-x}M_xO_3$ and $La_{1-x}Sr_xMnO_3$, it is found that the current density of oxygen reduction,

that is the catalytic activity, increased with an increase of the overlap integral, which is connected to promotion of the σ^* band formation as discribed in the former section. On the both electrodes, Tafel slope of 47 mV per decade was observed as shown in Figs. 4, 5 and 6. The value indicates that possible reaction pathes for oxygen reduction under an activation controlled condition may be either the one by Hoare [25,26] or Ives [26,27]. In either case, the following step is then the rate determing.

$$MO_2H + e \longrightarrow MO_2H^- \qquad (1)$$

where M represents an active site of the electrode. In the present case, M is a transition metal cation of the surface of the perovskite onto which one oxygen molecule adsorbs. Then, it seems to be reasonable that the catalytic acticity is controlled by the overlap integral between a transition metal ion and an oxygen ion nearest to it of the oxide.

Figs. 7 and 8 show the polarization curves of

Figure 8

oxygen reduction on $SrRuO_3$, $SrVO_3$ and $V_{0.2}Ti_{1.8}O_3$. It is found by comparing these figures with Figs. 4, 5 and 6 that a high overpotential was necessary for oxygen reduction on these oxides, although the catalytic

activity seemed to have some dependency on the pH values of electrolyte. In the both cases of $LaTiO_3$ and $SrFeO_3$ electrodes, no distinct reduction current of oxygen was observed. The π^* band formed by the M-O-M interaction in the conduction band in the cases of $LaTiO_3$, $SrFeO_3$, $SrVO_3$ and $SrRuO_3$, though the empty σ^* band is also formed in these oxides [13]. On the other hand, the conduction band of $V_{0.2}Ti_{1.8}O_3$ is the π^* band formed by M-M interaction and no σ^* band is formed [7]. On the basis of the above discussion, an important conclusion is drawn that the catalytic activity of the oxide having the σ^* coduction band is high, while those having the π^* conduction band is low or negligible.

From the above results, it is clear that the following two conditions must be fulfilled in order for a transition metal oxide to have a high catalytic activity. 1) The σ^* band must be formed, 2) It must have electrons. Importance of the first condition is demonstrated in the fact that the catalytic activity changed with the degree of substitution, x, in $La_{1-x}Sr_xMnO_3$ and $LaNi_{1-x}M_xO_3$. Importance of the second condition is observable in the fact that $LaTiO_3$, $SrFeO_3$, $SrVO_3$ and $SrRuO_3$, which have an empty σ^* band, showed low catalytic activities.

Qualitative relation between the catalytic activities

and the nature of the conduction band are summarized in Table 1.

Table 1

for a variety of transition metal oxides. In this table, the results obtained in this study as well as in other literatures are collected. From this table, it is noticed that the conduction band of transition metal oxides must satisfy the above mentioned two condition in order for the oxides to have a high catalytic activity for oxygen reduction.

Tseung and Bevan [19] reported that $La_{1-x}Sr_xCoO_3$ gave a so high catalytic activity as to give the equilibrium potential of oxygen at the potential expected by thermodynamics. According to Goodenough [28], the conduction band of this oxide is formed by overlapping the σ^* band with the π^* band. Hence, this oxide satisfies the above two conditions.

The two different bands have been proposed for the conduction band of Na_xWO_3. Mackintosh proposed the band formed by interaction between sodium orbitals [29], while Goodenough considered the π^* band formed by the M-O-M interaction [28]. The theory of π^* band seems to be more appropriate to understand the physical properties of Na_xWO_3. If the π^* band is the conduction band of Na_xWO_3, the catalytic activity for oxygen reduction must be low. It

was reported by Bockris et al. [30] that the catalytic activity of Na_xWO_3 is low, if the oxide is not doped with platinum.

Although NiO is a well known p-type semiconductor [31], the e_g orbital of Ni^{2+} is localized in the oxide [28]. However, the magnitude of the overlap integral of the e_g orbital of Ni^{2+} with the sp_σ orbital of oxygen ion in the oxide is equal to that of the critical overlap integral, that is, $\Delta^{\sigma}_{cac} \approx \Delta_c$, in the temperature range above the Neel point [32]. Therefore, formation of a partially filled σ^* band seems to be possible in temperatures above the Neel point. Then, NiO satisfies the above mentioned two necessary conditions. It was already reported that the catalytic activity of Li doped NiO became suddenly high above the Neel point [18].

There are two ways for an oxygen molecule to adsorb on an electrode, when it is electrochemically reduced. The side-on type adsorption, however, seems to be improbable in the following reason. On adsorption, oxygen will be adsorbed on sites in such a way that a transition metal ion is surrounded octahedrally. In the case when the side-on type adsorption takes place, the bond length between two oxygen atoms of an oxygen molecule must be stretched to long in order to fit the crystal structure of the electrode. For example, if side-on type adsorption takes place on the (110) plane, the bond length between oxygen atoms in an oxygen

molecule (1.2 Å) is much shorter than that between the nearest oxygen ions in the crystal (2.7 Å). Hence, the side-on type adsorption seems to be improbable on the perovskite structure. Therefore, end-on type adsorption is probable. On adsorption, the π^* orbital of an oxygen molecule, which is occupied by half with electrons and energetically highest [34], orients toward the e_g orbital of the transition metal ion. The probability for the e_g orbital to overlap with the π^* orbital of adsorbed oxygen will depend on the overlap integral, Δ^{σ}_{cac}.

The overlap integral of the π^* orbital of an oxygen molecule with t_{2g} orbital of a transition metal ion of the oxide will be very weak on the adsorption. Therefore, electrons in the σ^* band rather than π^* band seems to be more difficult to be transfered to the π^* orbital of an oxygen molecule. This is one possible reason why a transition metal oxide having the π^* conduction band shows a low or negligible catalytic activity for oxygen reduction.

TABLE 1. d-electron configuration of oxide and catalytic activity for oxygen reduction.

Oxide	d-electron configuration [13]	Conductivity 1)	Activity
$LaTiO_3$	$\pi^{*1}\sigma^{*0}$	metallic	negligible
$SrVO_3$	$\pi^{*1}\sigma^{*0}$	metallic	low
$SrFeO_3$	$t_\alpha^{*3}\pi_\beta^{*1}\sigma^{*0}$	metallic	negligible
$SrRuO_3$	$\pi^{*4}\sigma^{*0}$	metallic	low
$LaCrO_3$ [33]	$t^{*3}\sigma^{*0}$	semi	low
$La_{1-x}Sr_xCoO_3$ [19]	$t^{*6}\sigma^{*0}$ or $t^{*4}\sigma^{*2}$ (x=0) $\pi^{*n}\sigma^{*n}$ (x>0) 2)	semi-metallic	high
$La_{1-x}Sr_xMnO_3$	$t^{*3}eg^{*1}$ (x=0) ↓ $t^{*3}\sigma^{*1-x}$ (x>0)	semi-metallic	low (x=0) ↓ high (x>0)
$LaNiO_3$	$t^{*6}\sigma^{*1}$	metallic	high
$LaNi_{1-x}M_xO_3$ (M: Fe,Co)	$t^{*6}\sigma^{*1}$ (x=0) ↓ $t^{*6}eg^{*n}$ (x>0)	semi-metallic ?	high (x=0) ↓ low (x>0)
Na_xWO_3 [30]	$\pi^{*n}\sigma^{*0}$	metallic	low
$V_{0.2}Ti_{1.8}O_3$	π^{*n} 3)	metallic	low
Li-doped NiO [18]	eg^{*n} ($<T_N$) ↓ σ^{*n} ($>T_N$)	semi	relatively high ($<T_N$) ↓ very high ($>T_N$)

1) "metallic" and "semi" denote metallic conductivity and semiconductivity, respectively.

2) Overlap of π^* band with σ^* band.

3) This π^* band is formed by the interaction of M-M.

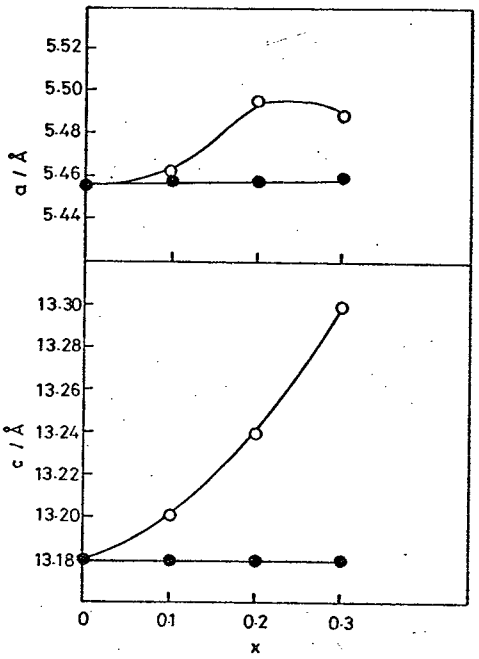

Fig.1. Lattice constants as a function of the degree of substitution. (O) $LaNi_{1-x}Fe_xO_3$, (●) $LaNi_{1-x}Co_xO_3$.

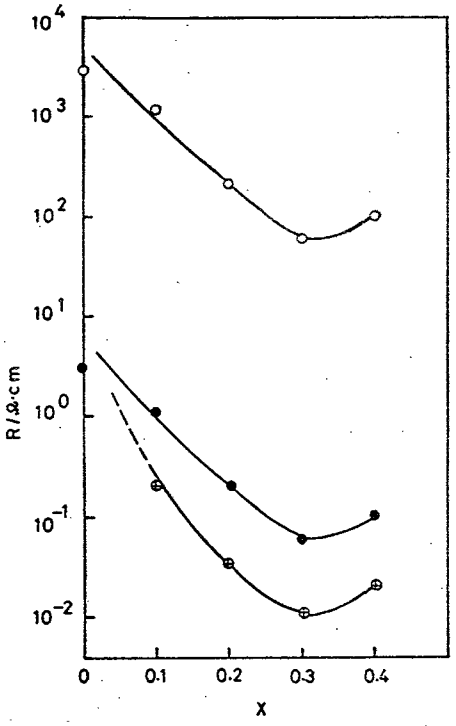

Fig.2. Resistivities of $La_{1-x}Sr_xMnO_3$ as a function of the degree of substitution, x. (O) sample bonded by a binder(12.5 wt%), (●) sintered disc, (⊕) values reported by Jonker[10].

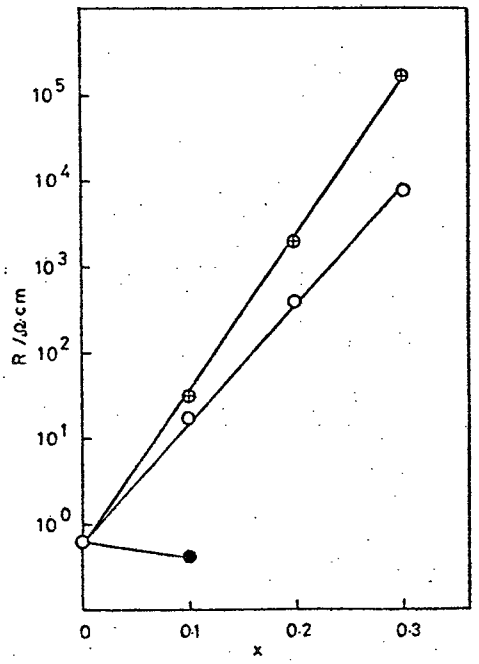

Fig.3. Resistivities as a function of the degree of substitution. (⊕) $LaNi_{1-x}Fe_xO_3$, (○) $LaNi_{1-x}Co_xO_3$, (●) $LaNi_{0.9}V_{0.1}O_3$.

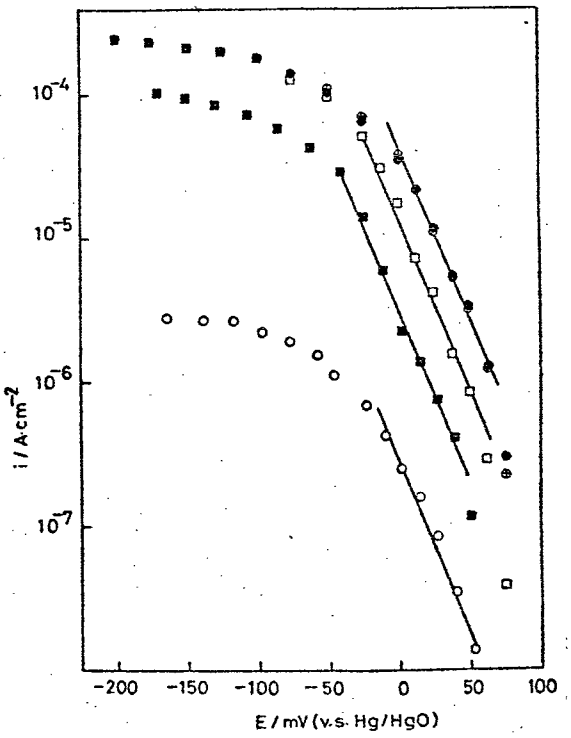

Fig.4. Current-potential curves of oxygen reduction in 1N-NaOH. (●) $LaNiO_3$, (⊕) $LaNi_{0.9}V_{0.1}O_3$, (□) $LaNi_{0.9}Fe_{0.1}O_3$, (■) $LaNi_{0.8}Fe_{0.2}O_3$, (○) $LaNi_{0.7}Fe_{0.3}O_3$.

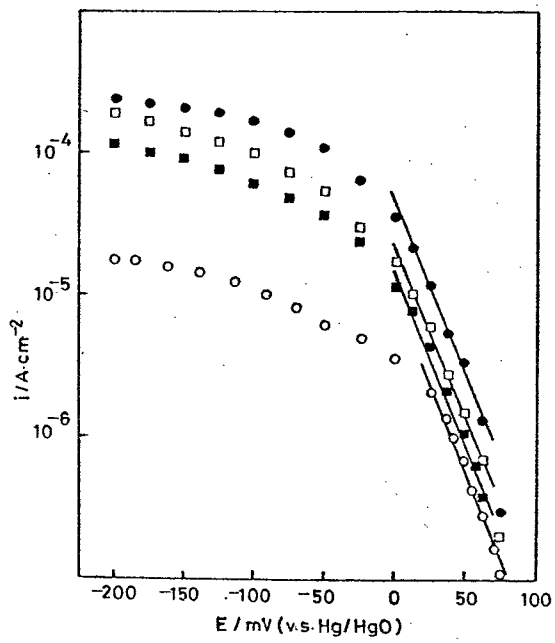

Fig.5. Current-potential curves of oxygen reduction in 1N-NaOH. (●) $LaNiO_3$, (□) $LaNi_{0.9}Co_{0.1}O_3$, (■) $LaNi_{0.8}Co_{0.2}O_3$, (○) $LaNi_{0.7}Co_{0.3}O_3$.

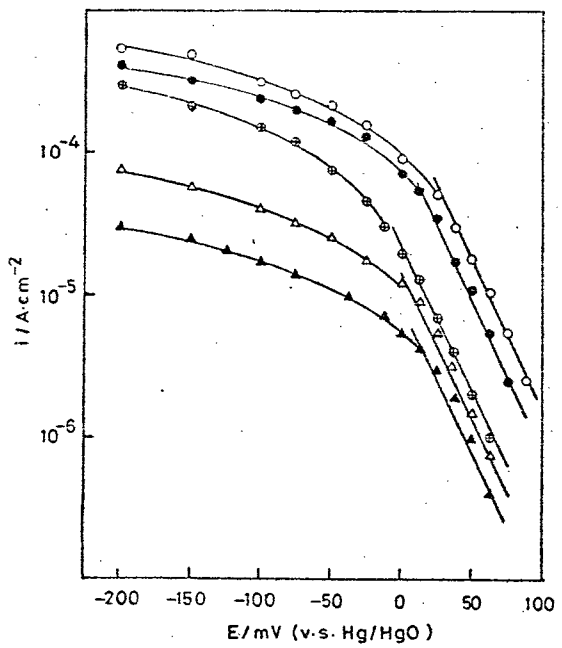

Fig.6. Current-potential curves of oxygen reduction on $La_{1-x}Sr_xMnO_3$ in 1N-NaOH. (○) x=0.4, (●) 0.3, (⊕) 0.2, (△) 0.1, (▲) 0.

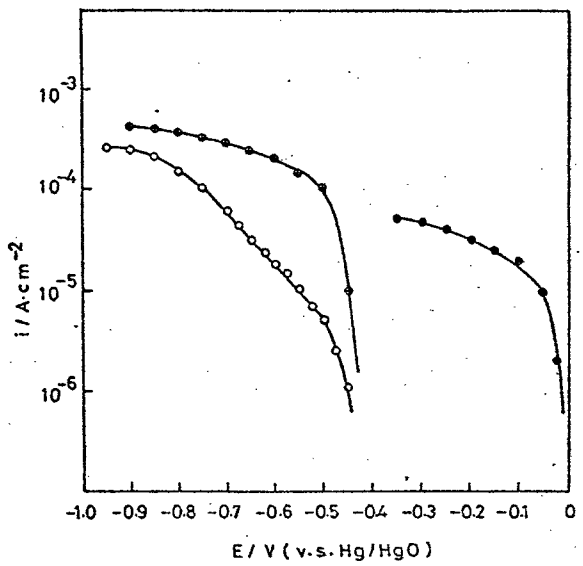

Fig.7. Current-potential curves of oxygen reduction in 1N-NaOH. (●) $SrRuO_3$, (⊕) $SrVO_3$, (○) $V_{0.2}Ti_{1.8}O_3$.

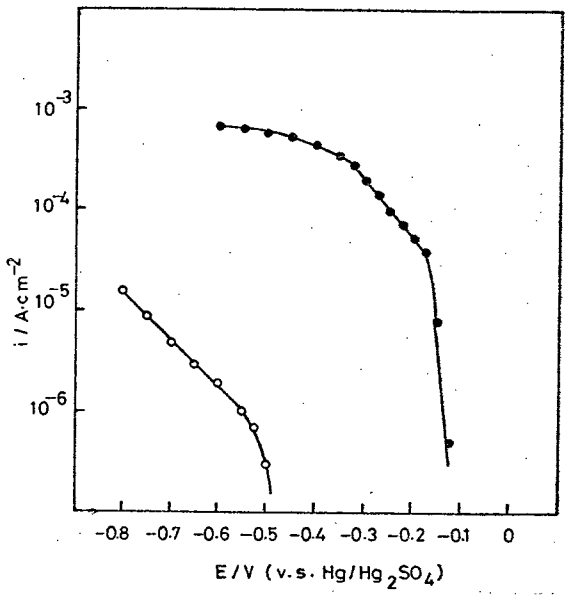

Fig.8. Current-potential curves of oxygen reduction in 1N-H_2SO_4. (●) $SrRuO_3$, (○) $V_{0.2}Ti_{1.8}O_3$.

CHAPTER IV

DEPENDENCY OF THE EXCHANGE CURRENT DENSITY OF OXYGEN REDUCTION ON THE RESISTIVITIES OF $La_{1-x}Sr_xMnO_3$ and $LaNi_{1-x}M_xO_3$ ELECTRODES

IV - 1. INTRODUCTION

In the preceding chapter, the following points were elucidated; (1) the catalytic activities of $La_{1-x}Sr_xMnO_3$ and $LaNi_{1-x}M_xO_3$ for oxygen reduction are influenced by the resistivity of the oxide which is determined by magnitude of the overlap integral, Δ^{σ}_{cac}, between the orbitals formed by an e_g orbital of a constitute metal ion and that by a sp_σ orbital of an oxygen ion ; (2) the activation controlled step of oxygen reduction seems to be $MO_2H + e \longrightarrow MO_2H^-$ in both oxides ; (3) an electron in the σ^* band of an oxide must transfer to the π^* orbital of an adsorbed oxygen molecule in this reaction step. Thire findings seem to suggest that the nature of electrons in the σ^* band, which is reflected in the resistivity of the oxides, influences on the rate of oxygen reduction. In this chapter, a relationship between the exchange current of oxygen reduction and the resistivity of the oxide are theoretically derived and is compared with experimental results already reported.

IV - 2. THEORETICAL ANALYSIS

Fig. 1 shows a schematic model of the electron transfer

Figure 1

in the rate determing step of oxygen reduction on $La_{1-x}Sr_xMnO_3$ and $LaNi_{1-x}M_xO_3$. This figure shows the case when the overlapping of the e_g orbital with the π^* orbital is relatively low. If the overlapping is very high, then the magnitude of the overlap integral should not exert an influence on the catalytic activity, because the probability of the electron transfer is unity in this case [35].

If an equation derived by Dogonadze et al. [36] for exchange current of a simple redox reaction is assumed to be applicable to the case of oxygen reduction, then the following equation holds for the oxygen reduction.

$$i_o=(e\delta/\hbar)\rho_f|L|^2(\pi kT/E_s)^{1/2}\exp(-E_s/4kT)\exp(-5e\psi/2kT) \qquad (1)$$

where L is the exchange integral between the e_g orbital of a transition metal ion and the π^* orbital of an oxygen molecule, ρ_f the density of states of electrons at the Fermi level, δ thickness of the Helmholtz double layer, E_s the reorganization energy of solvent, ψ the potential of the outer Helmholtz plane relative to a reference point in the bulk of solution, and e, $\hbar$, k and T have their usual meanings. The main factors to determine

i_o are ρ_f and L, since only the electrode material is different in the reaction system [37]. Therefore, the equation (1) can be simplified to equation (2).

$$i_o=\rho_f|L|^2C_1 \tag{2}$$

where $C_1=(e\delta/\hbar)(\pi kT/E_s)^{1/2}\exp(-E_s/4kT)\exp(-5e\psi/2kT)$

ρ_f and E_f are given by the following equations [38], respectively.

$$\rho_f=(V/2\pi^2)(2m^*/\hbar^2)^{3/2}E_f^{1/2} \tag{3}$$

$$E_f=(\hbar^2/2m^*)(3\pi^2N/V)^{2/3} \tag{4}$$

where m^* is the effective mass of electrons, V the volume of the unit cell and N number of free electrons.

Combining eq. (3) with (4), one obtains,

$$\rho_f=(3^{1/3}m^*V^{2/3}N^{1/3})/\pi^{4/3}\hbar^2 \tag{5}$$

Ratios of $V^{2/3}N^{1/3}$ of $LaNiO_3$ to that of $LaNi_{0.7}Co_{0.3}O_3$ and to that of $LaNi_{0.7}Fe_{0.3}O_3$ are $\sim$1.1 in both cases, if one choses numbers of free electrons in the e_g orbital of nickel in $LaNi_{1-x}M_xO_3$ as N. The ratio of $V^{2/3}N^{1/3}$ of $LaMnO_3$ to that of $La_{0.7}Sr_{0.3}MnO_3$ is again about 1.1. Therefore, eq. (5) is simplified to eq. (6).

$$\rho_f=C_2m^* \tag{6}$$

where $C_2=(3^{1/3}V^{2/3}N^{1/3})/\pi^{4/3}\hbar^2$

Replacing ρ_f in eq. (2) with eq. (6),

$$i_o=C_1C_2m^*|L|^2 \tag{7}$$

Although the overlap integral increases with an increase of the exchange integral [39], the relationship between them is not known exactly. However, the exchange integral in this case corresponds to the transfer integral, b_{ij},

which is approximated to be proportional to the overlap integral [40]. Therefore, for simplicity, let us assume that the exchange integral is a liner function of the overlap integral.

$$L=C_3 r \tag{8}$$

where r is the overlap integral between an e_g orbital of the transition metal ion of the electrode and the π^* orbital of an adsorbed oxygen molecule. As shown qualitatively in chapter III, it seems that r is proportional to the overlap integral, Δ^{σ}_{cac}, between the orbitals formed by the e_g orbital of the transition metal ion and the sp_σ orbital of the oxygen ion in the oxide.

$$r=C_4\Delta^{\sigma}_{cac} \tag{9}$$

Using the tight binding approximation [41], the relation between Δ^{σ}_{cac} and the effective mass of an electron in the σ^* band, m^*, is expressed by eq. (10).

$$\Delta^{\sigma}_{cac}=C\hbar\alpha^{-2}m^{*-1} \tag{10}$$

where C is a constant and α is the distance of the nearest neighbors. Although α depends on the size of the unit cell, the change of α in a perovskite oxide ABO_3 with promotion of the substitution to give $AB_{1-x}C_xO_3$ is not large. For example, ratio of α^2 of $LaNiO_3$ to that of $LaNi_{0.7}Fe_{0.3}O_3$ is no longer than 1.1. Therefore, eq. (10) is simplified to eq. (11).

$$\Delta^{\sigma}_{cac}=C_5 m^{*-1} \tag{11}$$

where $C_5=C\hbar\alpha^{-2}$

Using eqs. (8), (9) and (11), the exchange integral, L,

is expressed as a simple function of the effective mass of an electron, m^*, in the σ^* band.

$$L=C_3C_4C_5m^{*-1} \tag{12}$$

Replacing L in eq. (7) with eq. (12), the exchange current density of the oxygen reduction, i_o, is simplified to the following equation.

$$\begin{aligned} i_o &= C_1C_2C_3^2C_4^2C_5^2m^{*-1} \\ &= C_6m^{*-1} \end{aligned} \tag{13}$$

where $C_6=C_1C_2C_3^2C_4^2C_5^2$

The inversely proportional relationship of i_o to m^* in eq. (13) is due to that the effect of the overlap integral on i_o is stronger than that of the density of states, ρ_f. Combining eq. (11) with eq. (13),

$$i_o=\Delta_{cac}^{\sigma}C_5^{-1} \tag{14}$$

Eq. (14) shows quantitatively an enfluence of the overlap integral on the catalytic activity for oxygen reduction.

The resistivity of an oxide is represented by the following equation.

$$R=N^{-1}\mu^{-1} \tag{15}$$

where N is the concentration of carriers and μ is the mobility of the carriers. Since the carrier is electrons in the σ^* band and numbers of it seems to be almost proportional to the amount of the substitutive element, x, the resistivity of the oxide is determined mainly by the mobility of electrons. The relationship between the mobility and the effective mass was given for the case of the lattice scattering in the covalent bonding crystal, such as diamond, silicon

and gelmanium, by Seitze [42], and Bardeen and Schockley [43]. The equation given by Seitze is

$$\mu=6^{1/3}4^{-1}2^{1/2}P^{1/3}e\hbar^{2}k^{1/2}MC_f^{-2}T^{-3/2}\pi^{-5/6}\theta^{2}m^{*-5/2} \quad (16)$$

where P is the density of the unit cells of the lattice, θ the debye temperature, C_f a function of the Debye temperature originated from the Bloch function, and the other symbols have the usual meanings. If the mobility is assumed to be decisively determined by the effective mass, eq. (16) is simplified to eq. (17).

$$\mu=C_8 m^{*-5/2} \quad (17)$$

where $C_8=6^{1/3}4^{-1}2^{1/2}P^{1/3}e\hbar^{2}k^{1/2}MC_f^{-2}T^{-3/2}\pi^{-5/6}\theta^{2}$

This equation is derived by Bardeen and Schokley, too. In the case of the impurity scattering, however, Conwell and Weiskopf [44] proposed an another equation as shown in eq. (18) with the same assumption made in eq. (17).

$$\mu=C_8' m^{*-1/2} \quad (18)$$

In the cases of $La_{1-x}Sr_xMnO_3$ and $LaNi_{1-x}M_xO_3$, we cannot predict which equation is more appropriate to apply. Therefore, eqs. (17) and (18) are generalized to the following equation.

$$\mu=C_9 m^{*-n} \quad (19)$$

Combining eq. (15) with (19),

$$R=C_{10} m^{*n} \quad (20)$$

where $C_{10}=C_9^{-1}N^{-1}$

By combining eqs. (13) with (20), the dependence of the exchange current of oxygen reduction on the resistivity of the oxide is formulated as follows.

$$i_o=C_{11} R^{-1/n} \quad (21)$$

where $C_{11}=C_6C_{10}^{1/n}$

Therefore,

$$\ln i_o=(-1/n)\ln R + \ln C_{11} \qquad (22)$$

The equation (22) shows that the value of n in eq. (19) can be obtained from the slope of the line, if plots of $\ln i_o$ vs. $\ln R$ give a straight line.

IV - 3. RESULTS AND DISCUSSION

Figs. 2 and 3 show the exchange current densities of oxygen reduction on $La_{1-x}Sr_xMnO_3$ and $LaNi_{1-x}M_xO_3$ as a function of the degree of the substitution, x, which were obtained from the polarization curves in Figs. 4, 5

Figure 2

Figure 3

and 6 of chapter III. Fig. 4 shows plots of the exchange

Figure 4

current densities as a function of the resistivity of the electrode, for three kinds of the electrodes. The data of the resistivities used in this figure were already reported in the chapter III.

Good linearities of $\log i_o/\log R$ were obtained for a series of the perovskite oxides. In the case of $La_{1-x}Sr_xMnO_3$, the plots were made for the range of x from 0 to 0.3, because the resistivity seems to reflect the effect of the effective mass in this range as described in chapter III. The slope and n obtained are listed in Table 1. The present approach to give a theoretical background to the dependence of the exchange current density on the

Table 1

electrode conductivity may contain a detrimental defect in the point that derivation of eqs. (8) and (9) are based on rough approximation and that eq. (17) which is applicable to covalent bonding crystal is used in the perovskite oxide to derive a mobility-effective mass relation. However, the fact the value n found on $LaNi_{1-x}Fe_xO_3$ and $La_{1-x}Sr_xMnO_3$ were very close to the value predicted in eq. (17) is believed to support that the theoretical approach presented here is not unreasonable.

TABLE 1. Parameters of the relationship between the exchange current of oxygen reduction and the resistivities of electrodes.

Substances	Slope	n
$La_{1-x}Sr_xMnO_3$	-0.5	2.0
$LaNi_{1-x}Fe_xO_3$	-0.4	2.5
$LaNi_{1-x}Co_xO_3$	-0.18	5.6

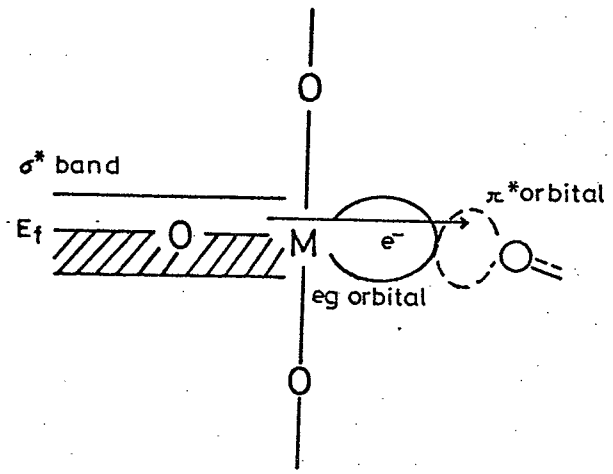

Fig.1. Model of the electron transfer of the rate determing step in oxygen reduction at $La_{1-x}Sr_xMnO_3$ and $LaNi_{1-x}M_xO_3$. M; transition metal ion, O; oxygen ion.

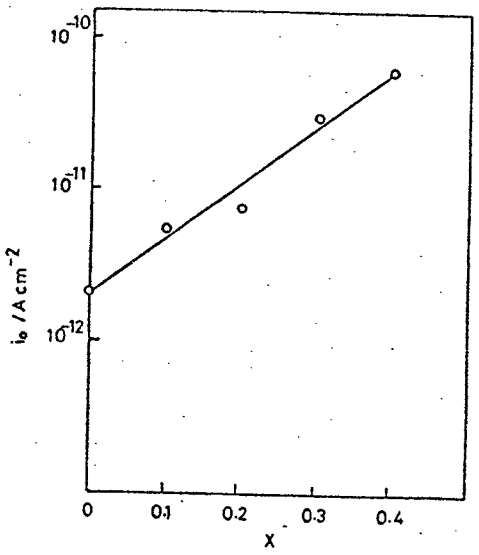

Fig.2. Exchange current densities of oxygen reduction on $La_{1-x}Sr_xMnO_3$ as a function of the degree of substitution, x.

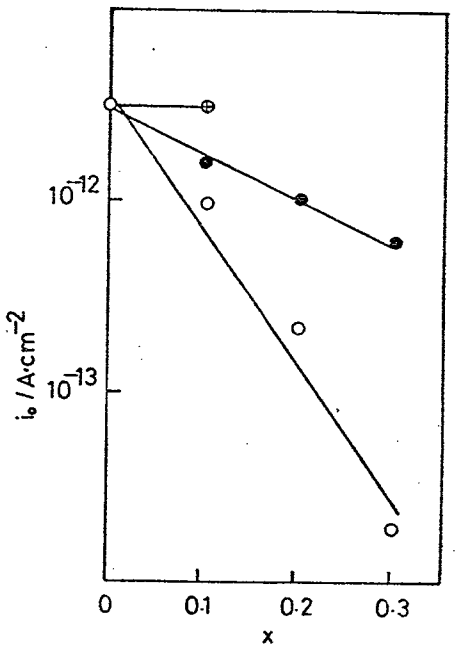

Fig.3. Exchange current densities as a function of the degree of substitution. (●) $LaNi_{1-x}Co_xO_3$, (○) $LaNi_{1-x}Fe_xO_3$, (⊕) $LaNi_{0.9}V_{0.1}O_3$.

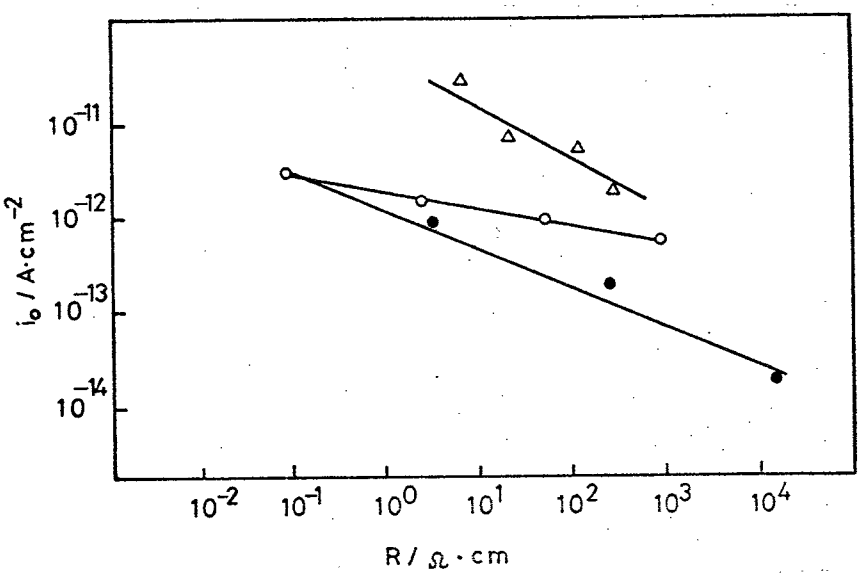

Fig.4. Plots of $\log i_o$ vs. $\log R$. (△) $La_{1-x}Sr_xMnO_3$, (○) $LaNi_{1-x}Co_xO_3$, (●) $LaNi_{1-x}Fe_xO_3$.

CHAPTER V

INFLUENCE OF PREPARATION CONDITION ON CATALYTIC ACTIVITY FOR OXYGEN REDUCTION OF LANTHANUM NICKEL OXIDE AND RELATED OXIDES

V - 1. INTRODUCTION

According to Goodenough [13], cations occupied A site in a perovskite type structure of ABO_3 negligibly influence the conductivity of the crystal on account of lacking interaction between the electron orbital of the A site ion and that of the oxygen ion. Hence, even if La^{3+} ions in $LaNiO_3$ are substituted by other lanthanoid elements, Ln, to form $La_{1-x}Ln_xNiO_3$, the electrocatalytic activity for oxygen reduction will be unchanged by the substitution. The present study was conducted to demonstrate the validity of this view.

Lanthanoid elements which can be substituted for lanthanum are limited to neodymium and samarium [8]. When the degree of substitution promotes, formation of foreign oxides as well as deformation of the perovskite structures are brought about. Therefore, the present chapter deals also with effects of crystal structures and deformation on catalytic activity of oxides for oxygen reduction.

V - 2. EXPERIMENTAL

$LaNiO_3$ were prepared by decomposition of nitrates, oxalates and carbonates, besides by the flux method. Oxides substituted some fraction of lanthanum with other lanthanoid elements such as samarium and neodymium were prepared by using a Na_2CO_3 flux at 850°C for two days.

A scanning electron microscope (SHIMADZU, EMX-SM) was employed in order to evaluate the crystal shapes of oxides.

Conventional pellets electrodes were prepared by the same manner as described in the former chapter to examine the nature of the electrocatalytic activity. Beside these electrodes, another two types of PTFE (polytetrafluoroethylene) bonded electrodes were prepared. One was prepared by pasting a mixture of PTFE ($14mgcm^{-2}$) and sample oxide ($56mgcm^{-2}$) onto a 100 mesh nickel screen and then by heating it at 250°C. This electrode was mounted in a glass tube with epoxy resin in such a manner that one side of the electrode is contacted with an electrolyte and the other side flowing oxygen of one atom pressure. The other was prepared by pasting a PTFE dispersion onto oxygen flowing side of the PTFE electrode, which was consisted of PTFE ($28mgcm^{-2}$) and $LaNiO_3$ ($56mgcm^{-2}$), and by heat treatment at 300°C. The former and the latter electrodes of the PTFE bonded electrodes are named as A and B type electrodes respectively in this chapter.

V - 3. RESULTS AND DISCUSSION

V - 3 - 1. Physical properties of oxides

Table 1 gives summary of products obtained, when trials were made to prepare $LaNiO_3$ by various methods.

Table 1

When flux methods were chosen, the flux of Na_2CO_3 gave the single phase of hexagonal $LaNiO_3$ at a lower temperature than that of K_2CO_3, on account of its lower melting point. $LaNiO_3$ having a cubic type structure was obtained by the decomposition method, as expected. However, a high temperature was necessary to obtain a single phase of $LaNiO_3$ than that reported by Foëx et al.(600°C) [45].

Resistivity and BET surface area in the table are given for as-producted oxides including foreign substances not intended, on account of difficulty of separation into individuals. Resistivity of single phase of $LaNiO_3$ prepared in the Na_2CO_3 flux decreased a little with increase of the reaction time. In the case of single phase $LaNiO_3$ prepared in the flux method, x ray diffraction patterns showed that diffraction peaks became sharp with an increase of the reaction time, indicating that the degree of crystalization increased with the reaction time.

When trials were made to prepare a single phase perovskite type oxide substituted some fraction of lanthanum of $LaNiO_3$ with neodymium, a foreign substance of neodymium nickel oxide was simultaneously produced when the degree of substitution intended was beyond 0.2. Similarly, in the case of substitution with samarium more than 0.1 fraction of lanthanum, products contained samarium nickel oxide. Fig. 1 shows x ray diffraction peaks of (100) and (012) planes of perovskite type oxide

Figure 1

produced. It was found from this figure that deformation of the perovskite type structure was promoted with the degree of substitution, x, and the rate of the deformation was higher for $La_{1-x}Sm_xNiO_3$ than for $La_{1-x}Nd_xNiO_3$. This observation was roughly in accord with Wold's results [8]. Easier substitution with neodymium than samarium is attributable to the fact that the ion radius of La^{3+} (1.346Å) is closer to that of Nd^{3+} (1.320Å) than Sm^{3+} (1.310Å) [22]. It was unsuccessful to separate mixed oxides into individuals when they were produced. Therefore, physical properties as well as electrochemical properties were obtained on the as-produced oxide. For simplicity of description, nominal composition intended, expressed in $La_{1-x}Ln_xNiO_3$, is used in this chapter even when mixed

oxides were produced.

It is noticed from the results in Table 2 that

Table 2

electrical conductivities of prepared oxides decreased with increase of x. The decrease seems to be resulted mainly from two causes. One is crystal deformation of the perovskite structure as stated above, and the other is existence of foreign oxides such as neodymium nickel oxide and samarium nickel oxide. The rate of the decrease with x in this case, however, was far less than that in the single phase perovskite type oxide substituted some fraction of nickel of $LaNiO_3$ with an other transition metal to give $LaNi_{1-x}M_xO_3$ as described in chapter 2. In the case of $LaNi_{1-x}M_x$, for example, substitution of Ni with Fe at x=0.3, brings increase of the resistivity by about four orders of magnitude, while in the case of mixed oxides expressed in $La_{0.7}Ln_{0.3}NiO_3$, where Ln is either Nd or Sm, the resistivity was only three or four times that of $LaNiO_3$, although an increasing trend of resistivity with x was noticeable.

If one takes into account that the resistivity is a measure of magnitude of the overlap integral between an electron orbital of nickel and of oxygen of the oxides [13], the overlap integrals of neodymium nickel oxide and

samarium nickel oxide as well as of perovskite type $La_{1-x}Ln_xNiO_3$ are judged to be comparable to that of $LaNiO_3$. This is an important conclusion on the basis of which electrocatalytic activity of the mixed oxide electrode is discussed.

Fig. 2 shows the crystalline forms obtained by a

Figure 2

scanning electron microscope of $LaNiO_3$, $La_{0.7}Nd_{0.3}NiO_3$ and $La_{0.7}Sm_{0.3}NiO_3$, prepared by the flux method, and of $LaNiO_3$ prepared by decomposition of nitrates at 950°C for one day. The crystalline forms of oxides prepared by the flux method were resemble with one another, and the particle sizes of crystals were several microns at largest. While, that of $LaNiO_3$ prepared by the decomposition of nitrates consisted of much fine particles of an order of 10^{-1} micron.

V - 3 - 2. Electrocatalytic activity for oxygen reduction

Cathodic polarization curves of oxygen are presented

Figure 3

in Fig. 3 for electrodes of cubic and hexagonal $LaNiO_3$, and of $La_{1-x}Nd_xNiO_3$. We see in this figure that reduction current on the cubic $LaNiO_3$ electrode is by one order

of magnitude higher than that on the hexagonal $LaNiO_3$. In the previous chapter, it was proposed that the overlap integral between the e_g orbital of nickel and the sp_σ orbital of oxygen is an important factor to determine the activity of the electrode for oxygen reduction. As the resistivity of cubic $LaNiO_3$ used as the electrode material (0.9 Ωcm) was comparable to that of hexagonal $LaNiO_3$ (0.8 Ωcm), the overlap integral is judged to be almost the same between the two electrodes. On the other hand, since the crystal of $LaNiO_3$ of the hexagonal type is the one distored only 43' in the (111) direction of the cubic cell, the catalytic activity seems to be scarcely influenced by the difference in structures. Therefore, a major part of the difference of the cathodic current of oxygen observed must be attributable to that of the surface areas of oxides as described above. The electrode of the single phase $La_{0.9}Nd_{0.1}NiO_3$ gave eventually the same polarization curves for oxygen reduction as that of $LaNiO_3$. Lattice constants of this oxide were judged to be the same as that of $LaNiO_3$. Considering that f electron orbitals of lanthanoid elements are localized in the oxides and has no influence on the overlap integral between nickel and oxygen, the result obtained was in accord with our expection.

Fig. 4 shows cathodic polarization curves of oxygen

reduction on $La_{1-x}Sm_xNiO_3$. All the Tafel slopes for

Figure 4

various $La_{1-x}Ln_xNiO_3$ electrodes were the same and 47mV per decade, as was observed at $LaNi_{1-x}M_xO_3$ electrodes as described in the previous chapter. Fig. 5 shows exchange

Figure 5

current densities as a function of the degree of substitution, x. It is shown in Figs. 3, 4 and 5 that the catalytic activity decreased with an increase of x in $La_{1-x}Ln_xNiO_3$ and that the degree of the decrease was larger for $La_{1-x}Sm_xNiO_3$ than for $La_{1-x}Nd_xNiO_3$. In our opinion, the fact that the current decrease with an increase of x in $La_{1-x}Ln_xNiO_3$ seems to be reasonable, because magnitude of the overlap integral between nickel and oxygen, the measure of which is the resistivity of the electrode, decreases with increase of x. If the overlap integral solely determines the catalytic activity, however, we should expect that the current is larger on $La_{1-x}Sm_xNiO_3$ than on $La_{1-x}Nd_xNiO_3$ at same value of x. The results are against this expectation. Therefore, we have to recognize that there is at least an another factor to control the electrocatalytic activity of the oxides.

It was noticed that deformation of the perovskite structure progressed with promotion of formation of the monoclinic oxide of neodymium nickel oxide or samarium nickel oxide, and that the rate of the deformation with x was larger for $La_{1-x}Sm_xNiO_3$ than $La_{1-x}Nd_xNiO_3$ on account of more difficulty of the substitution of La with Sm than Nd. It follows that these observations that the deformation of the perovskite structures as well as difference in the crystal structures are other important factors to determine the electrocatalytic activity of the electrode. Considering that there is large difference in the crystal structure between the perovskite and the monoclinic oxide such as samarium nickel oxide and neodymium nickel oxide, the catalytic activity for oxygen reduction of these monoclinic oxides may be different from that of the perovskite oxides.

If the monoclinic oxides are assumed to have no catalytic activity, then the catalytic activity of the electrode will be decreased in proportion to the amount of the monoclinic oxide in the electrode. The current decrease observed with an increase of the degree of substitution was, however, far more than that estimated by this assumption. On the estimation, it was assumed that Nd_2O_3 or Sm_2O_3 charged as the material in the synthesis was consumed to produce the monoclinic oxide when the degree of substitution was beyond x=0.1. Therefore, it is

suggested from this discussion that the deformation of the perovskite structure must decrease the catalytic activity of the electrode.

This suggestion is supported by the following results. When the current density for oxygen reduction was compared with one another at 0V on the single phase $LaNiO_3$ electrodes prepared by using Na_2CO_3 flux at different reaction time, $LaNiO_3$ prepared by one, three and seven day's reaction gave 20, 35 and 78 μAcm^{-2} respectively. As stated in the above section, crystalization of $LaNiO_3$ was promoted with increase of the reaction time. Therefore, it is clear that the catalytic activity for oxygen reduction was decreased with promotion of deformation of perovskite structures.

If the end-on type adsorption of an oxygen molecule as described in a previous chapter occurs, the e_g orbital of a transition metal ion, i.e., of Ni^{3+} in the present case, is very important for the catalytic activity of oxygen reduction. When the crystal structure of the perovskite is deformed, the direction of the d orbitals of a Ni^{3+} ion as well as the e_g orbital of it will become random. Then, the overlapping between the e_g orbital and the π^* orbital of oxygen molecule decreases delicately with promotion of the deformation of the perovskite structure, so that the catalytic activity decreases.

It should be stressed here, that the current

decrease by the deformation was not so that brought by substitution of the transition metal of $LaNiO_3$. For example, an electrode of the single phase of $LaNi_{0.7}Fe_{0.3}O_3$ gave a current decrease of two orders of magnitude by the substitution, while $La_{0.7}Sm_{0.3}NiO_3$ one order of magnitude.

Fig. 6 shows I/E curves of the A type electrode of $LaNiO_3$ in 30% KOH. The cubic lanthanum nickel oxide

Figure 6

prepared by the decomposition of nitrates showed a promising polarization behavior for oxygen reduction because of higher surface area than that prepared by the flux method.

Fig. 7 shows variation of oxygen reduction current

Figure 7

at 0.875V (vs. dhe) on the A and B type electrodes of $LaNiO_3$ which was prepared by the decompotion of nitrates ($950^{\circ}C$, 1day). A sharp drop at the A type electrode, which was observed after polarization for about ten hours, was attributable to penetration of the electrolyte into the oxygen flowing side of the electrode. The extent of the penetration of the electrolyte into the inside of the electrode was less at the B type electrode

than at the A type electrode by the fact that the former electrode was more tightly water-proofed with PTFE. The apparent activity for oxygen reduction was poor at the B type electrode as a matter of course. An initial rise of the current at the B type electrode with time is believed to be due to permeation of the electrolyte into the inside of the electrode. The succeeding gentle decrease was judged to be connected to a local penetration of the electrolyte into the oxygen flowing side of the electrode. The observation that the B type electrode gave an almost constant current over about a week except for the initial stage of the testing suggests that the catalytic activity for oxygen reduction will maintain over a long period if we can improve a fabrication technique of the electrode. It was reported that Co_2NiO_4 [23] and $Ln_{1-x}Sr_xCoO_3$ [46] showed a high catalytic activity for oxygen reduction at an initial stage of experiments, but the former and some of the latter oxides have a defect of instability in alkaline solutions. A composition change in the surface oxide into hydroxide was responsible for the instability of the former oxide, and formation of a large amount of oxygen vacancies within the crystal lattice for some of the latter oxides. In the case of $LaNiO_3$ electrode, formation of a large amount of oxygen vacancies, which will bring the destruction of the crystal structure,

is probable if it is polarized at potentials cathodic to about 0.55V (vs. dhe) as described in chapter II. However, it worked as an effective catalyst for oxygen reduction over a long period and the decomposition of the electrode was negligible so far as it was used in the potential region anodic to 0.55V (vs. dhe).

The high activity of the material with good stability and moderate price of starting materials are promising character of $LaNiO_3$ for practical use as a catalytst for oxygen electrode in an energy conversion system such as fuel cell. Figs. 6 and 7, however, show that some improvements should be made for particle sizes [47,48]of $LaNiO_3$ as well as fabrication technique of the electrode [49,50].

TABLE 1. Materials produced by different preparation conditions.

Preparation method	Starting material	Condition Time/day	Condition Temp./°C	Product	Resistivity /Ωcm	Surface area/m^2g^{-1}
Flux	La_2O_3 NiO (Na_2CO_3)	0.2		NiO, La_2O_3 $LaNiO_3$	750	
		1		$LaNiO_3$	1.2	0.5~0.7
		2,3	850		0.8	
		7			0.5	
		1	950	$NiLa_2O_4$ $LaNiO_3$	9.5	
	La_2O_3 NiO (K_2CO_3)	1	850	NiO, La_2O_3 $LaNiO_3$	78.0	
			950	$LaNiO_3$	3.1	
			1050		1.1	1.0
Decomposition of nitrates	$La(NO_3)_3 6H_2O$ $Ni(NO_3)_2 6H_2O$	2	600	NiO, La_2O_3	628	11.1
			850	$LaNiO_3$	1.8	4.7
		1			0.9	2.8
		2			0.6	2.5
	$La(NO_3)_3 6H_2O$ Ni carbonate	2	950	$LaNiO_3$	0.9	1.8
Decomposition of oxalates	$La_2(C_2O_4)_3 9H_2O$ $NiC_2O_4 2H_2O$	2	950	NiO, La_2O_3 $LaNiO_3$	196	2.9

TABLE 2. Materials produced by substitution of La with other lanthanoid elements.

Nominal composition	Products	Surface area/m^2g^{-1}	Resistivity/Ωcm
$LaNiO_3$	Perovskite	0.56	0.8
$La_{0.9}Nd_{0.1}NiO_3$	Perovskite	0.68	1.3
$La_{0.8}Nd_{0.2}NiO_3$	Perovskite, Neodymium nickel oxide	0.76	2.8
$La_{0.7}Nd_{0.3}NiO_3$	Perovskite, Neodymium nickel oxide	0.65	3.3
$La_{0.9}Sm_{0.1}NiO_3$	Perovskite, Samarium nickel oxide	0.92	0.6
$La_{0.8}Sm_{0.2}NiO_3$	Perovskite, Samarium nickel oxide	0.79	1.6
$La_{0.7}Sm_{0.3}NiO_3$	Perovskite, Samarium nickel oxide	1.67	2.8

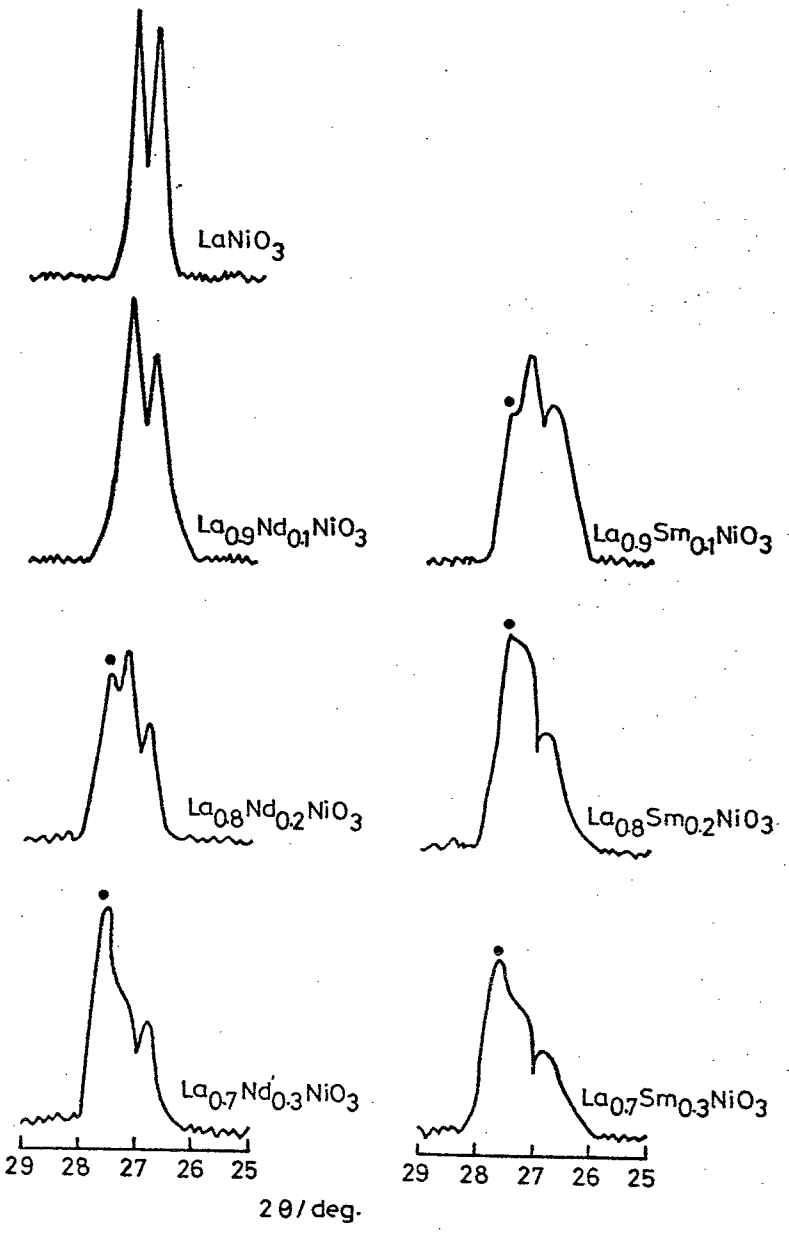

Fig.1. Deformation of x ray diffraction peaks of $La_{1-x}Ln_xNiO_3$ with promotion of substitution.
(●) neodymium nickel oxide or samarium nickel oxide.

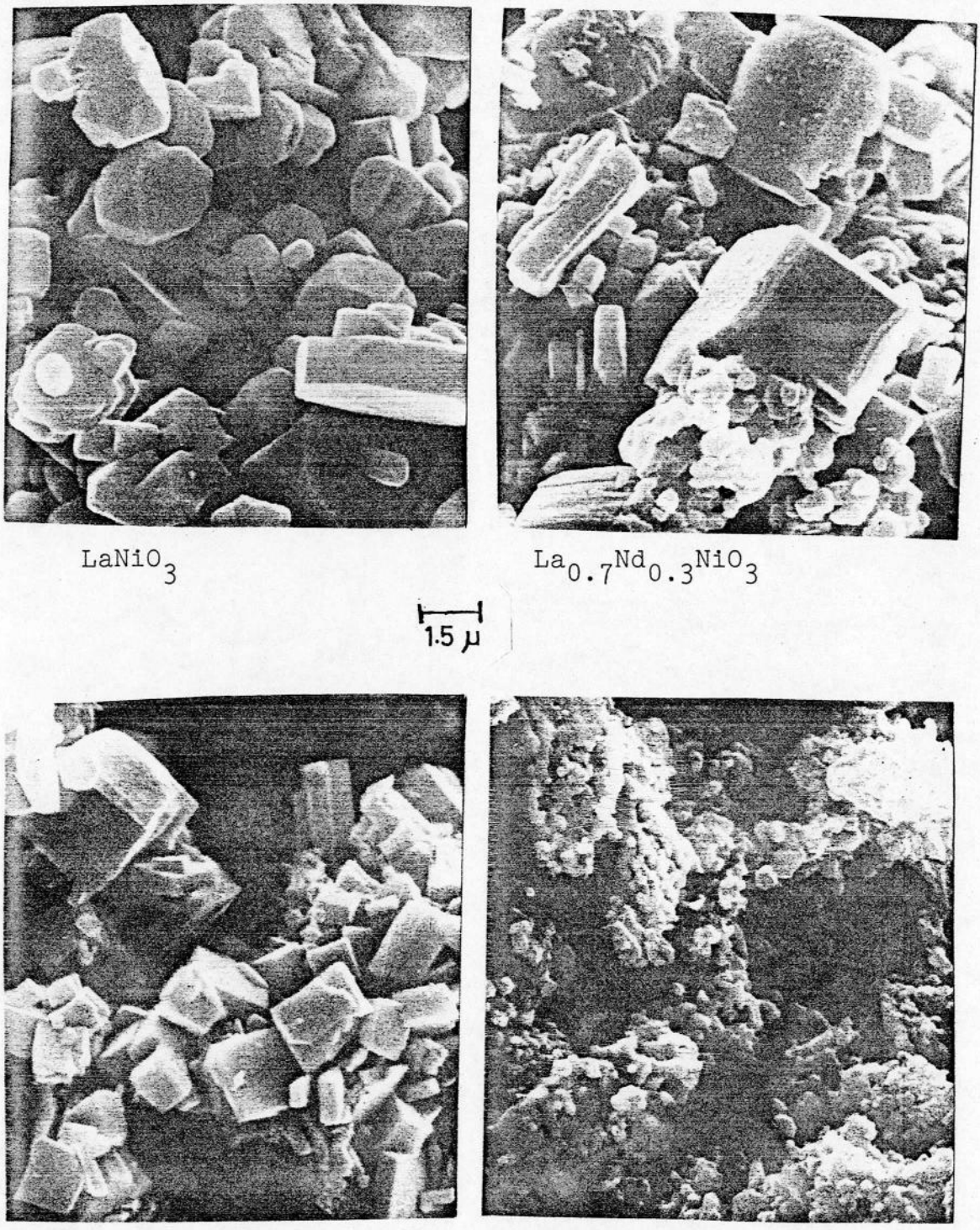

$LaNiO_3$

$La_{0.7}Nd_{0.3}NiO_3$

$La_{0.7}Sm_{0.3}NiO_3$

$LaNiO_3$ prepared by decomposition of nitrates

Fig. 2. Shapes of oxide crystals prepared.

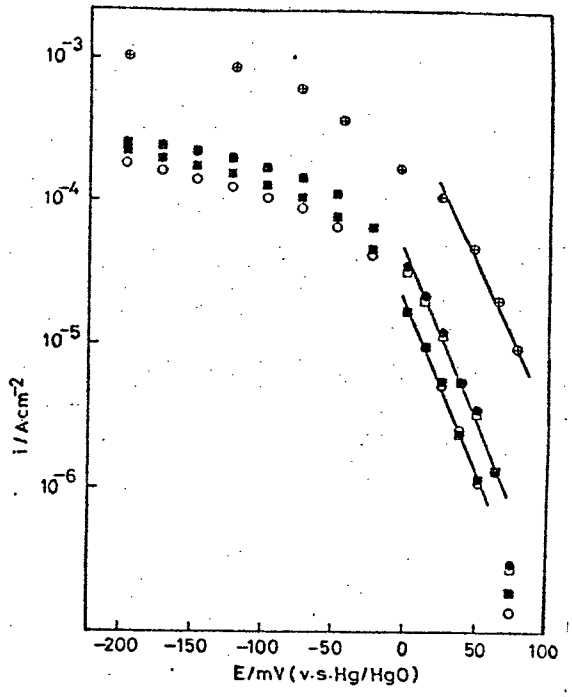

Fig.3. Current-potential curves of oxygen reduction in 1N-NaOH. (⊕) $LaNiO_3$ prepared by decomposition of nitrates (950°C, 1day), (●) $LaNiO_3$ prepared by the flux method (in Na_2CO_3, 850°C, 2days), (□) $La_{0.9}Nd_{0.1}NiO_3$, (■) $La_{0.8}Nd_{0.2}NiO_3$, (○) $La_{0.7}Nd_{0.3}NiO_3$.

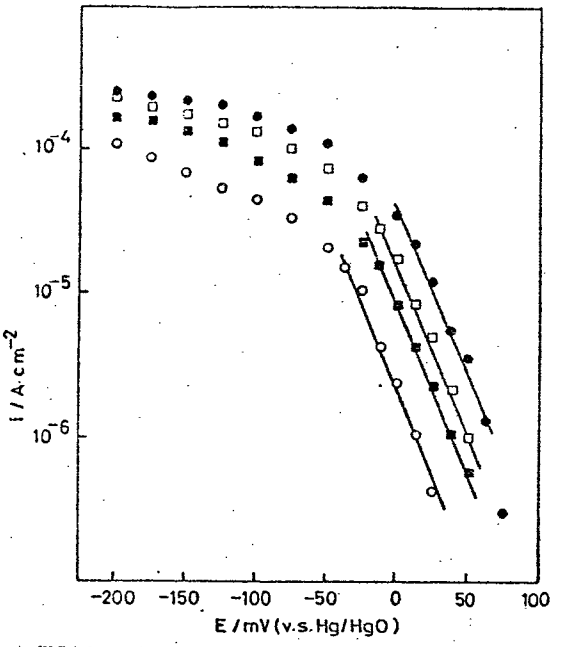

Fig.4. Current-potential curves of oxygen reduction in 1N-NaOH. (●) $LaNiO_3$, (□) $La_{0.9}Sm_{0.1}NiO_3$, (■) $La_{0.8}Sm_{0.2}NiO_3$, (○) $La_{0.7}Sm_{0.3}NiO_3$.

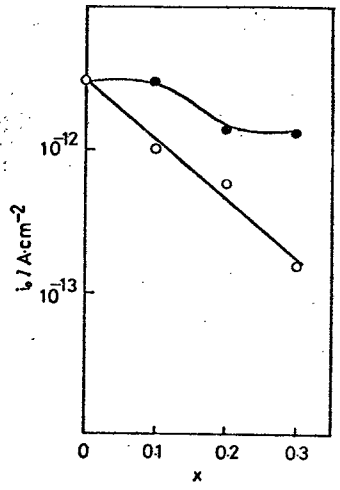

Fig.5. Exchange current densities as a function of the degree of substitution. (●) $La_{1-x}Nd_xNiO_3$, (○) $La_{1-x}Sm_xNiO_3$.

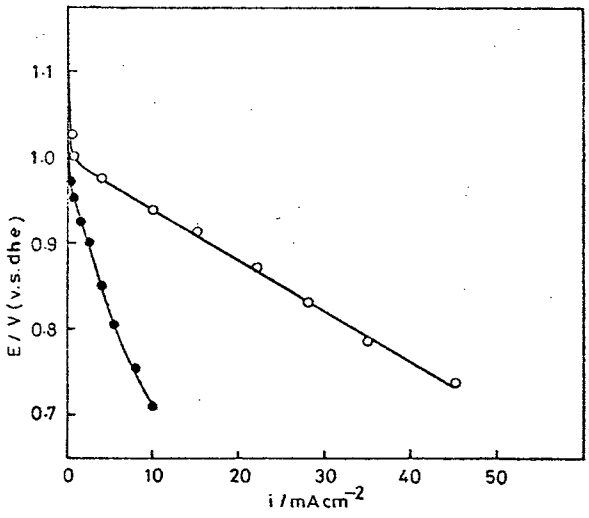

Fig.6. Current-potential curves of oxygen reduction on PTFE bonded electrodes in 30% KOH at 25°C. (○) $LaNiO_3$ prepared by decomposition of nitrates (950°C, 1day), (●) $LaNiO_3$ prepared by the flux method (in Na_2CO_3, 850°C, 2days).

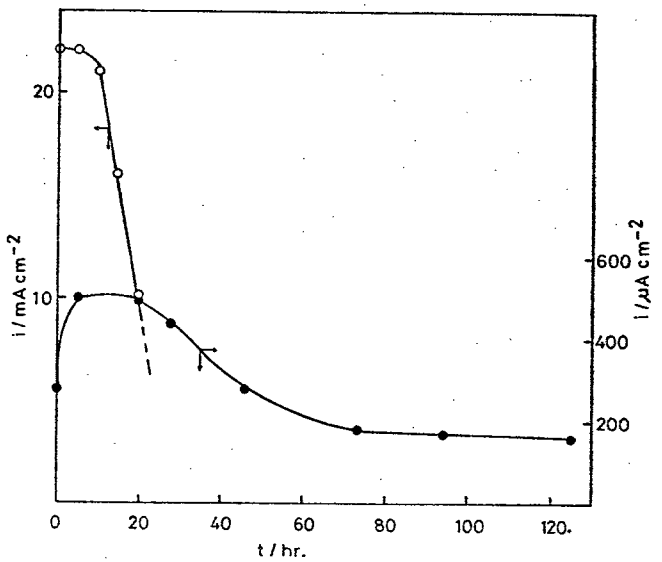

Fig.7. Variation of oxygen reduction current with time at 0.875V (vs. dhe) in 30% KOH at 25°C. (○) A type electrode, (●) B type electrode.

CHAPTER VI

CONCLUSION

The results of the present work are summarized as follows

1) The oxide with the perovskite type structure have relatively high activity for surface redox reactions of themselves in alkaline solution, which are resulted from exchange of the oxygen ions between the surface of the oxide and the electrolyte.

2) A conclusion was drawn that in order for a transition metal oxide to have a high catalytic activity for the cathodic reduction of oxygen, (i) it must have the σ^* band and (ii) the band must have electrons. This conclusion indicates that the e_g orbital of the transition metal ion on the electrode surface of the oxide is most important for the electron transfer in the oxygen reduction process.

3) A relationship between the exchange current density of oxygen reduction and the resistivities of the electrodes, i.e., $\ln i_o = (-1/n)\ln R + C$, were derived theoretically for $La_{1-x}Sr_xMnO_3$ and $LaNi_{1-x}M_xO_3$ by connecting an equation derived by Dogonadze and Chimadzev with the concept of the conduction mechanism of the transition metal oxides proposed by Goodenough. The derived relation was well in accord with the experimental results.

4) A fairly high current density of several ten $mAcm^{-2}$ was

obtained on $LaNiO_3$ prepared by the decomposition method. Although some improvements seem to be necessary for $LaNiO_3$ to have a practical significance as the electrocatalyst for oxygen reduction, a promising character was obtained.

ACKNOWLEDGEMENT

The auther is deeply indebted to Professor Hideo Tamura who kindly guided and encouraged me.

The auther is also indebted to Associate Professor Hiroshi Yoneyama for his valuable discussions and pertinent suggestions in the course of this thesis, and for kindful suggestions to prepare the manuscripts.

The auther is very grateful to Dr. Chiaki Iwakura and Mr. Osamu Ikeda for their helpful discussions throughout these works.

Finally, the auther wish to thank all the members of Tamura laboratory for their valuable suggestions and friendship.

REFERENCES

1) T. Takahashi and H. Iwahara, Denki Kagaku, 35 (1967) 433.

2) T. Kudo, H. Obayashi and T. Genjo, J. Electrochem. Soc., 122 (1975) 159.

3) M. Kestigian and R. Ward, J. Am. Chem. Soc., 76 (1954) 6027.

4) B. L. Chamberland and P. S. Danielson, J. Solid State Chem., 3 (1971) 243.

5) A. Callagham, C. W. Moeller and R. Ward, Inorg. Chem., 27 (1966) 1572.

6) G. H. Jonker, Physica (Utrecht), 20 (1954) 1118.

7) T. Kawakubo, T. Yanagi and S. Nomura, J. Phys. Soc. Japan, 15 (1960) 2102.

8) A. Wold, B. Post and E. Banks, J. Am. Chem. Soc., 79 (1957) 4911.

9) J. B. MacChesney, R. C. Sherwood and J. F. Potter, J. Chem. Phys., 43 (1965) 1907.

10) H. Yoneyama and H. Tamura, Bull. Chem. Soc. Japan, 45 (1972) 3048.

11) A. Kozawa and D. J. Brown, J. Electrochem. Soc., 113 (1966) 870.

12) D. M. MacArthur, J. Electrochem. Soc., 117 (1970) 422.

13) J. B. Goodenough, J. Appl. Phy., 37 (1966) 1415.

14) H. Obayashi, T. Kudo and T. Genjo, Japan. J. Appl. Phys., 13 (1974) 1.

15) D. B. Sepa, A. Damjanovic and J. O'M. Bockris, Electrochim. Acta, 12 (1967) 746.

16) A. C. C. Tseung, B. S. Hobbs and A. D. S. Tantram, Electrochim. Acta, 15 (1970) 473.

17) A. C. C. Tseung and B. S. Hobbs, Electrochim. Acta, 17 (1972) 1557.

18) H. L. Bevan and A. C. C. Tseung, Electrochim. Acta, 19 (1974) 201.

19) A. C. C. Tseung and H. L. Bevan, J. Electroanal. Chem., 45 (1973) 429.

20) W. J. King and A. C. C. Tseung, Electrochim. Acta, 19 (1974) 485.

21) W. J. King and A. C. C. Tseung, Electrochim. Acta, 19 (1974) 498.

22) M. Nakahira, Kessyo Kagaku, Kodanshya, Tokyo, 1975, p. 193.

23) H. Alt, H. Binder and G. Sandstede, J. Cata., 28 (1973) 8

24) H. Behret, H. Binder and G. Sandstede, Electrochim. Acta, 20 (1975) 111.

25) J. P. Hoare, J. Electrochem. Soc., 112 (1965) 849.

26) D. S. Gnanamuthu and J. V. Petrocelli, J. Electrochem. Soc., 114 (1967) 1036.

27) D. J. Ives and G. J. Janz, Reference Electrode-Theory and Practice, Academic Press, New York, 1961. p.365.

28) J. B. Goodenough, Progress in Solid-State Chemistry, vol. 5, Pargamon Press, 1971, p. 145-399.

29) A. R. Mackintosh, J. Chem. Phys., 38 (1963) 1991.

30) J. O'M. Bockris and J. McHardy, J. Electrochem. Soc., 120 (1973) 61.

31) S. van Houten, J. Phys. Chem. Solids, 17 (1960) 7.

32) J. B. Goodenough, Mat. Res. Bull., 2 (1967) 165.

33) D. B. Meadowkroft, Nature, 226 (1970) 847.

34) G. H. Olivé and S. Olivé, Angev. Chem. Int. Ed. Engl., 13 (1974) 29.

35) V. G. Levich, Advances in Electrochemistry and Electrochemical Engineering, vol. 4, Interscience, New York, 1967, p. 249-371.

36) R. R. Dogonadze and Yu. A. Chizmadzev, Dokl. Akad. Nauk SSSR., 145 (1962) 849.

37) M. V. Vojnovic and D. B. Sepa, J. Chem. Phys., 51 (1969) 5344.

38) C. Kittel, Introduction to Solid State Physics, Jhon Wiley and Sons, Inc., New York, 1971 p. 247-249.

39) M. Oiwa, Shyotō Ryoshi Kagaku, Kagakudojin, Kyoto, 1972, p. 149.

40) J. B. Goodenough, Mat. Res. Bull., 2 (1967) 37.

41) C. Kittel, Introduction to Solid Physics, Jhon Wiley and Sons, Inc., New York, 1971, p. 714-718.

42) F. Seitz, Phys., 73 (1948) 549.

43) J. Bardeen and W. Schokley, Phys. Rev., 80 (1950) 72.

44) E. Comwell and V. G. Weisskopf, Phys. Rev., 77 (1950) 388.

45) M. Foëx, A. Mancheron and M. Line, Compt. Rend., 250 (1960) 3027.

46) H. Obayashi and T. Kudo, Denki Kagaku, 44 (1976) 503.

47) A. C. C. Tseung and H. L. Bevan, J. mater. sci., 5 (1970) 604.

48) W. E. Kuhn and H. Lamprey, Ultrafine Particles, New York, 1963.

49) K. V. Kordesh, Fuel Cells, Academic Press, New York and London, 1963, p. 345.

50) L. M. Litz and K. V. Kordesh, Fuel Cell Systems, Amer. Chem. Soc., Washington, D.C., 1965, p. 166.